



Computational Hemodynamics in Human Vasculature: A Review on Role of Rheology, Multiphase Flow, and Fluid–Structure Interaction

Sumant R. Morab, Atul Sharma^{*}  and Janani S. Murallidharan

Abstract | Efficient and accurate computational model for blood flow dynamics (hemodynamics), is essential for determining optimal treatment strategy, diagnosis, and pathology identification of cardiovascular diseases (CVDs). The focus of the present review paper is to discuss on critical aspects of hemodynamics. Various numerical methods for computational hemodynamics are examined—addressing three key modeling choices. First, the relevance of non-Newtonian hemorheological models in varying vascular conditions is presented. Second, an assessment of single-phase versus multiphase modeling's validity, for different arterial geometries, is presented. Lastly, investigation on the impact of arterial wall elasticity on blood flow patterns is carried out and a discussion on the necessity of fluid–structure interaction (FSI) model is presented. By surveying diverse scenarios of blood flow modeling, presented in recent literature, it is observed that non-Newtonian behavior significantly impacts severely stenosed arteries or those with low diameters and Womersley numbers, while larger arteries exhibit characteristics similar to Newtonian fluids. Differences between single-phase and multiphase modeling vary with arterial configurations, showcasing notable particle migration effects in curved and branched arteries. Additionally, arterial wall elasticity's influence varies across scenarios—highlighting the importance of FSI, particularly in diseased states. The article identifies crucial areas for future research to enhance CFD-based hemodynamic modeling, emphasizing the integration of multiphase simulation with non-linear elastic arteries, considering surrounding tissue effects in FSI, innovating patient-specific CAD geometries, and developing faster computational techniques.

Keywords: Cardiovascular diseases, Computational fluid dynamics, Fluid–structure interaction, Non-Newtonian

1 Introduction

Cardiovascular diseases (CVDs) encompass a range of conditions affecting the heart and blood vessels. They are a leading cause of mortality

worldwide, claiming millions of lives annually. According to a recent survey by American Heart Association¹, CVDs account for nearly 18 million deaths each year—representing about 31% of all

¹ Department of Mechanical Engineering, Indian Institute of Technology Bombay, Mumbai, Maharashtra 400076, India.
*atulsharma@iitb.ac.in

global deaths. Among these fatalities, *Coronary Artery Disease (CAD)*^{A2}, stroke, heart failure, and hypertensive heart disease are prevalent contributors. These statistics underscore the critical need for innovative approaches in managing and preventing CVDs.

Computational modeling of blood flow, within the human vasculature has emerged as a pivotal tool in modern medicine. It basically involves a computer program-based solution of governing physics-based mathematical model, to obtain blood flow velocities and pressure at numerous discrete locations and time instants inside human vasculature. This technology offers numerous advantages, which significantly impact the diagnosis, treatment, and understanding of cardiovascular conditions. One key advantage lies in the realm of surgery planning, where computational models can aid in selecting appropriate implants.^B The model involves simulation of blood flow patterns and predicting the behavior of various prosthetic devices within the vascular system³. This enables surgeons to personalize treatments, optimizing the choice of implants for individual patients and enhancing surgical outcomes. Moreover, these models play a pivotal role in the development of new diagnostic devices^{4,5}. By simulating blood flow under various conditions, researchers can design and test diagnostic tools that accurately detect anomalies in circulation—enabling earlier and more precise diagnosis of cardiovascular issues. Understanding the possibility of plaque growth is another crucial aspect facilitated by computational modeling. These models simulate the flow of blood, highlighting regions susceptible to plaque^C accumulation^{6,7}. This knowledge allows for better prediction of potential blockages, aiding in preventive measures and targeted treatments to mitigate the risk of arterial blockages and related complications. Furthermore, computational models provide insights into hemodynamics^{D8–11}, elucidating the complex interplay between blood flow and vessel structure. This understanding helps in predicting potential complications post-surgery, optimizing treatment strategies, and advancing our comprehension of cardiovascular physiology¹².

Computational fluid dynamics (CFD) for modeling blood flow in human vasculature involves several key steps¹³. First, in the pre-processing step, geometric reconstruction of the vasculature is done using idealized geometries or from medical imaging data like magnetic resonance imaging (MRI)^E or computed tomography (CT) scans.^F Thereafter, the geometry is meshed, that involves subdividing the flow domain into small elements for calculations. Boundary conditions like blood pressure and flow rates are set and governing fluid flow equations are solved using numerical methods. Finally, in the post-processing step, the results are analyzed to understand blood flow patterns, pressure distributions, and shear stresses within the vessels. The analysis leads to crucial insights for medical interventions and device design. Before delving further into computational models along with their challenges and current state of art, it is essential to understand human vasculature and complexities which may arise in defining the governing physics-based mathematical model.

The human vasculature system comprises arteries, veins, and capillaries—forming an intricate network responsible for transporting blood throughout the body, as shown in Fig. 1 (Chapter 2—Tu et al.¹⁴). Arteries carry oxygenated blood away from the heart, branching into smaller vessels called arterioles. On the other hand, veins return de-oxygenated blood back to the heart, with venules connecting to larger veins. Vessels vary in diameter, from large arteries like the aorta (2 cm) to tiny capillaries (10 μm)¹⁵, and are crucial for nutrient exchange. The Reynolds number Re ,^G which signifies the flow regime, varies widely within the vasculature, ranging from 20 (arterioles) to 2000 (aorta) due to changes in velocity and diameter. Arteries possess elasticity, allowing them to expand and contract in response to blood flow changes and maintain a steady circulation. Further, blood is a complex fluid, comprising of plasma, red blood cells (RBCs), white blood cells (WBCs), and platelets¹⁶, as shown in Fig. 2. Its behavior is challenging to model computationally due to its non-Newtonian nature,

^A Narrowing or blockage of the coronary arteries, which supply blood to the heart muscle.

^B Tiny, expandable metal mesh tubes that are placed inside a blocked artery during angioplasty.

^C Fatty deposit made up of cholesterol, cellular waste products, calcium, and fibrin, blocking blood flow in arteries.

^D Study of blood flow dynamics within animal vessels.

^E Use of a strong magnetic field and radio waves to create detailed images of the organs and tissues within the body. MRI can help with viewing injuries, tumors, certain heart problems, and more.

^F Diagnostic imaging exam that uses X-ray technology to produce images of the inside of the body.

^G Non-dimensional flow parameter signifying ratio of inertial to viscous forces. Calculated as $Re = UD/\nu$, where U is characteristic flow velocity, D is artery diameter, and ν is kinematic viscosity of blood.

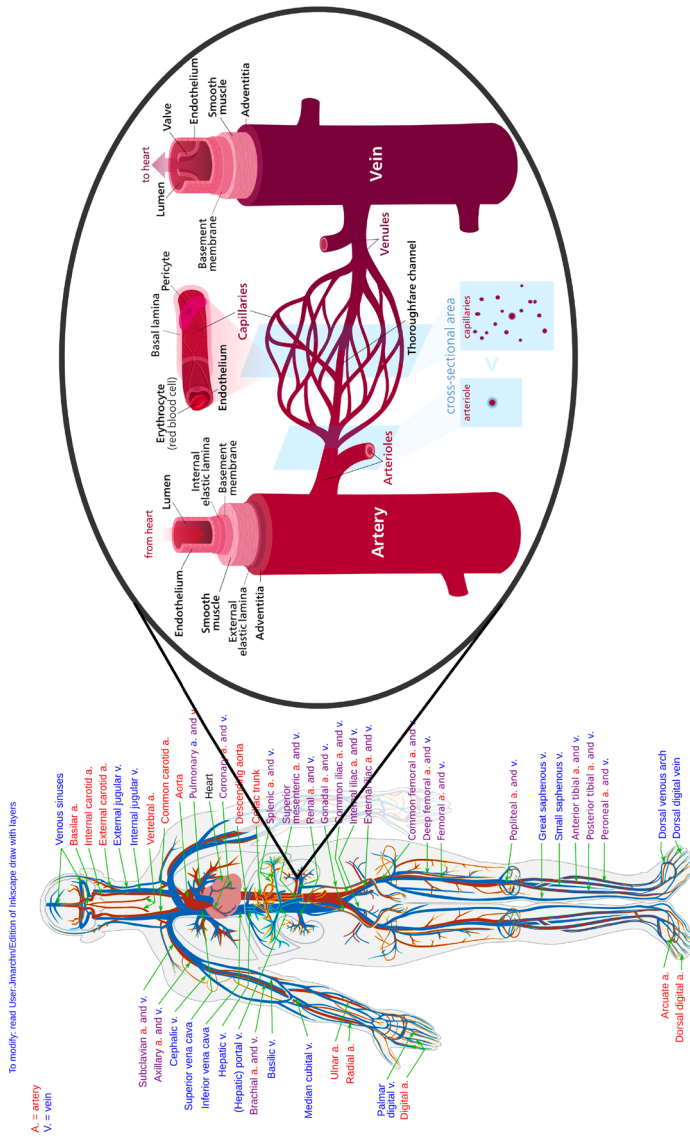


Figure 1: Human vasculature system consisting of arteries, veins, and connecting capillaries (adapted from [7] and modified suitably).

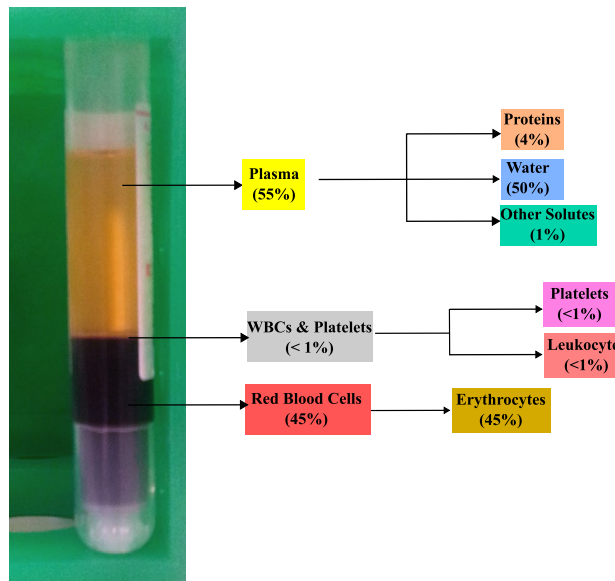


Figure 2: Composition of human blood (modified from source: Zuzanna K. Filutowska, <https://commons.wikimedia.org/w/index.php?curid=29764058>).

exhibiting varying viscosity and flow properties under different conditions. Moreover, accounting for factors like the pulsatile nature of blood flow, vessel compliance,^H and the dynamic interaction between blood and vessel walls adds complexity to accurate computational modeling of blood flow in these intricate networks. Achieving precise simulations necessitates sophisticated models that consider these multifaceted characteristics.

The above discussion shows that there are multiple physics (involving two-phase composition, flexibility of artery, elasticity of RBCs, and shear-dependent viscosity^I) which need to be considered for computational solutions. After the rapid development in computer hardware and processing speed during recent decades, CFD modeling for physiological flows (air flow in respiratory system, blood flow in circulatory system) has progressed to a large extent. Summary of literature survey on CFD studies for blood flow modeling in human vasculature is presented in Table 1. The table shows that different authors have worked on different arterial systems with some assuming single phase, rigid walls, and constant viscosity. It becomes important to understand which assumptions can be made for a particular artery under study so as to obtain accurate results with optimal computational cost.

^H Ability of arteries to expand and contract in response to changes in blood pressure, allowing them to accommodate varying blood flow.

^I Measure of a fluid's resistance to deformation under stress.

In this regard, there are several papers^{2,6,18,19} which discuss the latest trends in *physiological* modeling and the realistic computational models. However, as per our knowledge, many of these are restricted to one particular artery type or deal with a single type of modeling variation (example, single and multi-phase, rigid and compliant). In an effort to address this disparity, the present article undertakes a comprehensive examination of blood flow modeling techniques and attempts to offer recommendations regarding assumptions that can be made for relevant flow and geometric parameters.

The present article provides a comprehensive literature review on three crucial choices (during computational modeling of human vasculature)—single-phase versus multi-phase flow, Newtonian versus non-Newtonian hemorheology, and the need for modeling fluid–structure interaction (FSI). First, the review is focused on whether the intricate motion of RBCs within blood vessels requires a multi-phase model or if single-phase modeling suffices to capture the essence of blood rheology and hemodynamic variables. Further, the review explores significance of shear rate-dependent blood viscosity and the role of red blood cell (RBC) elasticity in shaping hemorheological^J dynamics. Finally, the influence of flow-induced periodic arterial deformation-based vibration on hemodynamics is presented, which leads to further investigation into the most

^J Study of the fluid properties of blood and its characteristics.

Table 1: Summary on CFD-based modeling of blood flow in various human vasculature system.

Author (year)	CFD study performed	Physics involved and computational tool	Observations
Wu et al. ²⁰ (2015)	Pulsatile blood flow in idealized stenosed and dilated coronary arteries	single-phase blood flow + linear elastic artery deformation—ANSYS CFX	Stenosis in coronary artery has enhanced flow resistance and vulnerability to plaque growth as compared to dilatation
Lorenzini et al. ²¹ (2008)	Pulsatile blood flow in idealized different shaped arterial constriction	single-phase non-Newtonian blood-flow with rigid artery wall—COMSOL multi-physics	Slope of constriction caused larger variation in hemodynamics as compared to other changes
Rayz et al. ²² (2008)	MR-based patient-specific pulsatile blood flow in cerebral aneurysm	Single-phase blood flow with rigid artery wall—ANSYS Fluent	Good comparison between CFD and phase-contrast MRI results for velocity contours
Dennis et al. ²³ (2017)	CT-based Patient-specific pulsatile blood flow in intracranial aneurysm ¹⁰	Single-phase blood flow with rigid artery wall—ANSYS Fluent	Simulation results are very sensitive to the solver setting. A high-fidelity solver with CFL < 0.1 necessary for obtaining accurate results
Qiao et al. ²⁴ (2019)	CT-based Patient-specific pulsatile blood flow in aortic dissection ¹¹	Two-phase non-Newtonian blood-flow with compliant artery (linear material model)—ANSYS + in-house solver	Hemodynamic parameters like Oscillatory Shear Index (OSI) changed between single and two-phase for regions of non-uniform RBC distribution
Chen et al. ²⁵ (2021)	Pulsatile blood-flow in left coronary artery (LCA)	Single-phase non-Newtonian blood-flow with compliant artery. Tracked LDL using a transport equation—MIMICS + ANSYS	LDL deposition coincides with regions of low wall shear stress (WSS). Higher blood pressure increases LDL uptake from flowing blood in the arterial wall
Wu et al. ²⁶ (2020)	Pulsatile blood flow in idealized curved coronary artery	Single-phase non-Newtonian with Philips diffusive flux model for RBC concentration. Artery wall—rigid	RBCs migrate toward the inner surface of curvature—correlating with sites of plaque formation. Minor changes in hemodynamics
Bruneau et al. ²⁷ (2023)	CT-based patient-specific pulsatile blood flow in eight different intracranial aneurysms	Single-phase non-Newtonian with high-fidelity FSI model for artery vibration capture	FSI model throws light of acoustic murmurs heard in a clinical setup. High frequency signals captured due to higher order structural solver

¹⁰ Bulge or ballooning in a blood vessel within the skull

¹¹ Medical condition involving a tear in the inner layer of the aorta

suitable material models for the studied artery network. Through an interconnected exploration of these inquiries, this review seeks to highlight the state of the art while navigating the challenges that underlie computational hemodynamics in human vasculature.

The present article is on reviewing and comparing computational modeling techniques and assumptions for blood flow in human vasculature. Our main focus is on arteries since major abnormalities occur here and veins follow similar modeling techniques with outline as follows: Sect. 2 presents the governing equations for simulating single/two-phase blood flow in flexible artery, along with the coupling between artery vibrations and blood flow parameters. Section 3 presents the variations in blood flow modeling using single and two-phase approach, along with suitable conditions where single-phase approach can yield accurate results. In order to close the stress tensor discussed in mathematical model, Sect. 4 discusses the rheology of blood and different non-Newtonian models of varying complexities, which can be used to model the viscosity of blood and elasticity of RBC particles. Further, Sect. 4.3 presents a comparison of Newtonian and non-Newtonian models for different arteries and flow conditions so as to gage the necessity of such complex models. After discussing blood flow modeling and variations of viscous stress formulation, Sect. 5 attempts to answer the last research question regarding necessity of including fluid–structure interaction (FSI) in the numerical model. In this section, a comparison of rigid modeling and compliant artery modeling (with linear and non-linear material) is provided so that readers can understand suitability of lower end models depending on the case being studied.

2 Mathematical Model

Blood is commonly treated as single fluid with homogeneous distribution of all particles due to similar properties of RBCs and plasma. However, in several cases, this assumption does not remain valid and blood is treated as mixture of mainly plasma and RBC since platelets and WBCs constitute to only 1% of total volume. Considering this into account, mathematical formulation for blood flow, artery deformation, and the resulting fluid–structure interaction are presented in separate subsections below.

2.1 Hemodynamics

The governing compressible Navier–Stokes equation for two-phase mixture of RBC and plasma is given as follows²⁸: Continuity:

$$\frac{\partial}{\partial t}(\epsilon_k \rho_k) + \nabla \cdot (\epsilon_k \rho_k \vec{u}_k) = 0 \quad (1)$$

Momentum:

$$\begin{aligned} \frac{\partial}{\partial t}(\epsilon_k \rho_k \vec{u}_k) + \nabla \cdot (\epsilon_k \rho_k \vec{u}_k \vec{u}_k) \\ = -\epsilon_k \nabla p + \nabla \cdot \bar{\tau}_k + \epsilon_k \rho_k \vec{g} \\ + \sum_{l \neq m}^n \beta_{lm}(\vec{u}_l - \vec{u}_m) + \vec{F}_k \end{aligned} \quad (2)$$

Equation of state:

$$p = \rho_{\text{mix}} R T_{\text{mix}} \quad (3)$$

where $k = (\text{plasma, RBCs})$, ρ is the density, ϵ is the volume fraction of each phase ($0 \leq \epsilon_k \leq 1$), T is the temperature, ϕ_{mix} is the mixture property, and \vec{u} is the velocity. Further, p is the pressure common to both phases, $\bar{\tau}$ is the viscous stress tensor,^K \vec{g} is the gravity force, n is total number of phases (two here), and \vec{F} is the shear lift force; found using Saffman–mei inertial lift force model²⁹. Further, β_{lm} is the interphase momentum exchange coefficient^L with l and m being the indices of plasma and RBCs, respectively (since there are only two phases involved here). It should be noted that the volume fractions of all phases must sum to unity i.e., $\epsilon_{\text{plasma}} + \epsilon_{\text{RBC}} = 1$. For each phase k , the stress tensor $\bar{\tau}$ is given as:

$$\begin{aligned} \bar{\tau}_k = \epsilon_k \mu_k \left(\nabla \vec{u} + (\nabla \vec{u})^T \right) \\ + \epsilon_k \left(z_k - \frac{2}{3} \mu_k \right) \nabla \cdot \vec{u} \bar{I} \end{aligned} \quad (4)$$

where μ_k and z_k are the shear and bulk viscosity of each phase, respectively. The bulk viscosity z_k is usually treated as zero. Shear viscosity is considered constant for a Newtonian fluid assumption whereas it is modeled as function of hematocrit (RBC concentration) and shear rate for non-Newtonian flow. Discussion on rheology of blood is presented separately in Sect. 4. Further, the

^K Tensors can be thought of as multidimensional arrays of numbers that transform in a specific way under changes of coordinates.

^L In multiphase flow, especially when dealing with two or more phases (such as gas–liquid or liquid–solid), the movement and interaction between these phases affect their velocities and distribution. The momentum exchange coefficient helps describe how momentum is transferred between these phases during their interaction.

interface momentum exchange coefficient β_{lm} can be determined as follows:

$$\beta_{lm} = \frac{3}{4} C_d \frac{\rho_{\text{plasma}} \epsilon_{\text{plasma}} \epsilon_{\text{RBC}} |\vec{u}_{\text{plasma}} - \vec{u}_{\text{RBC}}|}{d_{\text{RBC}} \phi} \quad (5)$$

where $d_{\text{RBC}} \approx 8 \text{ mm}$ (RBC diameter), and $\phi \approx 1$ (shape factor). The drag coefficient C_d is given by:

$$C_d = \begin{cases} \frac{24}{Re_p} \left(1 + 0.15 Re_p^{0.687}\right) & Re_p < 1000 \\ 0.44 & Re_p \geq 1000 \end{cases} \quad (6)$$

where

$$Re_p = \frac{\rho_{\text{plasma}} d_{\text{RBC}} |\vec{u}_{\text{plasma}} - \vec{u}_{\text{RBC}}| \phi}{\mu_{\text{plasma}}}$$

Thus, using the above constitutive relations (Eqs. 4, 5, 6), the mass and momentum conservation equations (Eqs. 1, 2) can be obtained in a closed form.

It should be noted that these equations can be further simplified by using single phase approximation and incompressibility.^M In this approach, the whole blood is considered to be a single fluid with constant density and constant/spatio-temporally varying viscosity. Thus, for single fluid model, the generalized governing equations presented above can be simplified by setting $\epsilon_1 = 1$ and $\epsilon_i = 0$ ($i \neq 1$). Further, the interface momentum exchange can also be ignored. The new set of governing equations for incompressible blood flow are given as follows:

$$\begin{aligned} \nabla \cdot \vec{u} &= 0 \\ \rho \left(\frac{\partial \vec{u}}{\partial t} + (\vec{u} \cdot \nabla) \vec{u} \right) &= -\nabla p + \bar{\tau} \end{aligned} \quad (7)$$

where $\bar{\tau}$ is modeled using Eq. (4) with $k = \text{blood}$. This approach of blood flow modeling has been used over a long time and is validated with in vivo experiments and MRI measurements^{22,30}. The single fluid modeling works, especially in case of large arteries with high Re flows due to the fact that RBCs are very small in size ($8 \mu\text{m}$) as compared to artery diameter (2 mm–2 cm) and move freely with plasma, without actually imparting any effect on plasma. If objective of the study is to understand blood flow patterns and trend of hemodynamic parameters (so as to see which areas are more prone to damage), the single fluid approach is more suitable as it takes less computational time. A comparison of multiphase and

single fluid models are presented elaborately in Sect. 3.

2.2 Artery Deformation-Based Structural Dynamics

Arteries in human vasculature are found to be flexible in nature and act as capacitor which store blood during systolic phase by expanding and release it during diastolic phase by contracting. This helps in reduction of high temporal variation of blood pressure. Thus, it becomes important to model arterial deformations in order to obtain hemodynamic variables accurately. For a general compressible solid, the Lagrangian framework-based^N governing momentum equations is given as:

$$\rho_s \frac{\partial^2 \vec{d}}{\partial t^2} = \nabla \cdot \bar{\tau}_s + \vec{f}_s^B \quad (8)$$

where ρ_s is the density, \vec{d} is the displacement vector, $\bar{\tau}_s$ is the Cauchy stress tensor, and \vec{f}_s^B is the body force vector for solid element s . There are two types of non-linearity while modeling structural deformation. First is a relation between stress tensor $\bar{\tau}_s$ and strain ϵ_s , which is decided by choice of linear or non-linear material modeling. Second is the choice of relation between strain ϵ_s and displacement gradients which lead to geometric linear or non-linear model. Generally, material non-linearity is decided by the response of material to applied load, i.e., the resulting stress–strain graph while geometric non-linearity is considered when structural displacements are larger ($> 10\%$ of length scale). For compliant artery and veins-based circulatory system, a detailed discussion on need for structural modeling along with suitable material modeling schemes are presented in Sect. 5.

2.3 Fluid–Structure Interface Coupling

Once arterial deformations are modeled along with blood flow, it becomes utmost important to consider the effect of arterial deformation on the flow and flow-induced load on the artery. Thus, there is a two-way coupling between fluid and structural dynamics that needs to be ensured through suitable interface coupling given as follows:

^M Property of having negligible changes in density under normal variations in pressure or temperature.

^N The Lagrangian framework follows individual particles or elements within a system as they move through space and time. It tracks the properties of these elements as they evolve.

1. *Continuity of velocity* At the fluid–solid interface if , velocity of the fluid flow $\vec{u}_{f,if}$ is equal to the structural velocity $\vec{u}_{s,if}$ given as

$$\vec{u}_{f,if} = \vec{u}_{s,if} \quad (9)$$

where the subscript f and s represent fluid and solid respectively.

2. *Force balance* For the bodies to be in equilibrium, a balance between hydrodynamic and elastic forces is ensured normal to the interface given as

$$[\bar{v}_{s,if}] \cdot \hat{n}_{s,if} + [\bar{v}_{f,if}] \cdot \hat{n}_{f,if} = 0 \quad (10)$$

where at the interface, \hat{n}_{if}^s and \hat{n}_{if}^f represent

outward normal unit vector at the solid and fluid subdomains, respectively.

Commonly, the above interfacial boundary conditions are implemented with fluid-dynamic pressure and viscous stress for obtaining structural displacements, which in turn is used to enforce the continuity of the fluid velocity at the interface³¹.

3 Computational Hemodynamics: Whether Multiphase Model is Required?

As discussed in the introduction (Sect. 1), blood consists of particles (RBCs, WBCs, and platelets) that are suspended in liquid plasma. Since plasma constitutes more than 50% volume fraction and RBCs around 45%, blood can be modeled using the Eulerian–Eulerian two-phase model; described in Jung et al.²⁸. The corresponding governing equations are already presented in Sect. 2 (Eqs. 1, 2). However, RBCs can be considered to have similar properties of plasma and a single fluid approach may also be used, especially when shear rate and diameter are higher (governing equations presented in Sect. 2). Thus, it becomes important to understand the right choice of computational approach for the artery being studied and also desired application for which simulations are being carried out. In order to address this issue, a literature survey of single-fluid and multiphase (mostly RBC–plasma mixture) models along with a discussion on suitability of single versus multi-phase modeling, are presented below.

Although single-fluid models have advantages, the movement of particles (specifically RBCs) within the blood cannot be understood using such models—discussed in Sect. 2. It is

known that atherosclerosis^O initiates in humans with monocytes adhering to the endothelium,^P yet despite decades of research⁷, the exact trigger for this response remains unknown. It tends to localize near arterial side branches and the inner curvature, where hemodynamic stresses significantly influence the early stages of CVDs. Predicting particle accumulation could be an initial step toward comprehending atherogenesis,^Q aligning with clinical observations. Thus, in order to understand the pathogenesis (process by which a disease or disorder develops) behind atherosclerosis and to correlate it with hemodynamic parameters, it becomes essential to understand the concentration difference in particles and/or to see where the particles are staying for long time. A multiphase simulation is required to achieve the above objective. Gidaspow³² provides a comprehensive description of multiphase flow, highlighting the primary distinction from a single-phase model—the inclusion of volume fraction for each phase and mechanisms facilitating the exchange of mass, momentum, and energy between these phases. A brief review of multiphase modeling for blood-flow simulations and observations reported are presented below.

Jung et al.²⁸ presented a multiphase transient non-Newtonian three-dimensional CFD model, for pulsatile flow in a *curved coronary artery*. Their model (similar to Eqs. 1–6) was formulated using the concepts developed during 30 years of biomedical CFD modeling and 20 years of multiphase research, especially in Eulerian–Eulerian phase modeling. Their simulations showed that RBC volume fractions were highest on the inside curvature, and secondary flows weakened during diastole—increasing RBC buildup. They reported that particulate buildup on inside curvature correlates with lower wall shear stress. Further, two-phase non-Newtonian viscosity model also predicted a greater shear thinning as compared to single-fluid model. These predictions provide insight into how blood-borne particulates interact with artery walls and hence, multiphase models have relevance for understanding atherogenesis since clinical observations show that atherosclerotic plaques generally form on the inside curvatures of arteries. On a similar line, Kim et al.³³ investigated the influence of mechanical

^O A chronic and progressive condition characterized by the buildup of plaque inside the arteries.

^P The endothelium is a thin layer of flat cells that lines the inner surface of your blood vessels.

^Q Atherogenesis is the complex process by which fatty deposits, called plaques, build up inside the walls of arteries.

factors on the hemodynamics of a curved coronary artery—using multiphase non-Newtonian fluid simulations of pulsatile flow. It was reported that the high hematocrit levels induce secondary flow, and RBC viscosity as well as Wall Shear Stress^R (WSS) vary with hematocrit level. It was argued by the authors that although all models have a good approximation in blood-flow behavior, the multiphase non-Newtonian viscosity model is optimal—to demonstrate effects of changes in hematocrit and provides a better simulation of realistic blood flow analysis. Huang et al.³⁴ discussed the use of a multiphase kinetic theory model to simulate pulsatile flow in a *coronary artery*. They showed that the multiphase kinetic theory model accurately computes viscosity and migration of red blood cells. WSS and its gradients were highest on inside area of maximum curvature. Thus, the multiphase kinetic theory model has been shown to compute correctly the viscosity of RBCs and their migration away from vessel walls: the Fahraeus–Lindqvist effect³⁵.

While multi-phase blood flow simulations offer detailed analysis, our survey reveals minimal differences in WSS compared to single-phase models, especially for large arteries (≥ 2 mm). This suggests that, for these vessels, prominent hemodynamic parameters can be calculated accurately using single-phase models, while accurate physical description of hemodynamic characteristics necessitates multiphase/multi-component modeling. However, multiphase may be necessary to dynamically model the growth of stenosis since plaque growth is caused by WSS variation, which in turn varies with plaque build-up level. For example, Jung et al.³⁶ used multiphase modeling to analyze hemodynamics in a non-uniform right coronary artery. They computed RBC build-up and WSS variation along its length. Interestingly, despite non-uniform geometry, regions with high curvature showed both increased RBC build-up and WSS. This suggests factors like flow reversal and secondary flow might also play a role in RBC distribution. Such simulations are complex to model^{37–39} and require larger computational cost and are currently under development.

The above discussed multiphase models consider two different mass and momentum conservation equations, which need to be solved simultaneously. They also involve several

constitutive relations for shear lift force, interface momentum exchange—making the computations complex and time-consuming. A relatively simpler approach involves using a single phase approach, with fluid as plasma, and modeling RBC (Hematocrit) concentration using Philips diffusive flux model⁴⁰—a scalar transport equation. Thus, one needs to solve single set of mass and momentum equations along with an equation for hematocrit given as

$$\frac{\partial \phi}{\partial t} + (\vec{u} \cdot \vec{\nabla})\phi = -\nabla(N_c + N_\mu + N_g) \quad (11)$$

where ϕ is the volume fraction of RBCs. Further, N_c , N_μ , and N_g are the contributions to the diffusive flux from particle collisions, spatial variation of viscosity, and gravitational force, respectively. These terms can be expanded in terms of geometric and flow parameters as:

$$\begin{aligned} N_c &= -a^2 \phi K_c \nabla(\dot{\gamma} \phi); \\ N_\mu &= -a^2 \phi^2 \dot{\gamma} K_\mu \nabla(\ln \mu); \\ N_g &= \frac{2}{9} \phi \frac{\mu_{f0}(1-\phi)}{\mu} \frac{a^2(\rho_{s0} - \rho_{f0})}{\mu_{f0}} g \end{aligned} \quad (12)$$

where a is the radius of RBC (assumed sphere), $K_c \approx 0.43$, and $K_\mu \approx 0.62$ are empirically determined coefficients. Further, ρ_{f0} and ρ_{s0} are the density of plasma and RBC, respectively.

Using the above model, Wu et al.²⁶ presented numerical simulation of blood flow in a sudden expansion channel and a curved coronary artery, focusing on the movement of red blood cells and the formation of atherosclerotic plaque. First, they showed that velocity profiles in sudden expansion flow agree with experiments. For the idealized curved coronary artery, they found that the RBCs move toward and concentrate near the inner surface, where the viscosity is higher and the shear stress lower similar to the phenomenon observed using Eulerian–Eulerian multiphase model. Thus, for micro-level arterial network, the diffusive flux model can be successfully applied. A similar model was used by Yadav et al.⁴¹ to simulate blood flow even at mesoscale^S (10–300 μm). Through comparison with experiments, it was shown that such models could accurately predict flow patterns for smaller capillary vessels. Although the above works

^R WSS refers to the force per unit area exerted by the flowing blood against the endothelial layer (inner lining) of the vessel walls. It is calculated as $WSS = \mu \frac{\partial u_t}{\partial y}$, where u_t is velocity component tangential to artery wall and n is the normal distance from artery wall.

^S Mesoscale flow refers to fluid motion occurring at an intermediate scale between the microscale (very small, such as molecular or particle-level interactions) and macroscale (larger, such as the scale of weather systems or ocean currents). Validity of continuum hypothesis starts to break down in these scales.

are mostly for coronary artery and microchannels, several other studies have performed multiphase simulations in *carotid*^{42,43} and *femoral*^{44,45} arteries also.

Based on literature survey for single and multiphase blood-flow modeling, it can be observed that hemodynamic parameters like WSS, Oscillatory Shear Index (OSI),^T and wall shear stress gradient (WSSG) can be accurately calculated using single fluid model, especially for larger arteries like carotid, femoral, and aorta. However, the particle motion cannot be tracked accurately (even using Lagrangian tracking through single fluid results) and there may be errors $\geq 5\%$ for small arteries and veins. Thus, a judicious choice is needed to decide whether single fluid model is sufficient or multiphase (computationally more expensive) is necessary-based on the application of the study.

4 Role of Rheology of Blood and its Constituents on Computational Hemodynamics

Apart from the multiphase versus single phase modeling discussed in the above section, determination of appropriate model for viscous stress tensor $\bar{\tau}$ is equally important. As discussed in Sect. 1, the blood consists of various small particles like RBC, WBC, and platelets-suspended in liquid plasma. The interaction between RBCs and plasma leads to major changes in the effective viscosity of the blood flowing in artery of diameter D . At very small shear rate^U $\dot{\gamma}$, RBCs aggregate with each other forming cylinder-like structures—called as *rouleaux*, which resist the blood flow and lead to increased viscosity. As the $\dot{\gamma}$ increases, these stacked-up RBCs slowly disaggregate, which allows the blood to move freely; thus resulting in reduction in viscosity. With increasing $\dot{\gamma}$, after a critical shear rate $\dot{\gamma}_c$, the RBCs completely disaggregate into single structures, align with the flow and make the blood to have constant viscosity μ_∞ . Thus, it can be concluded that blood is a shear-thinning fluid.^V This is

^T OSI is a parameter used in the study of fluid dynamics, particularly in the context of blood flow, which describes the directional changes in shear stress on the endothelial lining of blood vessels during the cardiac cycle.

^U Shear rate is a fundamental parameter used to describe the rate at which adjacent layers of fluid move relative to each other in a flow field. It represents the velocity gradient or the change in velocity per unit distance between fluid layers.

^V Shear-thinning fluid is a type of non-Newtonian fluid whose viscosity decreases as the shear rate increases i.e., as more force or shear stress is applied, it becomes easier to deform or flow.

verified by an experiment performed by Chien⁴⁶ where normal RBCs suspended in plasma (NRP), and normal and hardened RBCs suspended in 11% albumin-Ringer (NRaR, HRaR) solution are subjected to varying shear rate inside a tube, and corresponding viscosity is measured using rheometer. Figure 3a shows the variation of viscosity with shear rate for these three different type of solutions. It can be observed that the NRPs, which indicate actual blood have a shear thinning property i.e, the viscosity is found to decrease with shear rate and attain a constant value after $\dot{\gamma} = 100 \text{ s}^{-1}$. For hardened and/or albumin-Ringer solution suspended RBCs, the aggregation is not possible and hence a constant viscosity is observed.

Apart from shear rate, viscosity is also affected by the hematocrit (RBC concentration) and the diameter of artery. The hematocrit increases the viscosity while the diameter change has a non-linear effect. At very small diameters ($d < d_1$), the viscosity increases exponentially with reduction in diameter. This is because the diameter of artery becomes close to RBC diameter and hence a very high resistance for fluid flow is observed. At $d > d_1$, with increasing diameter, the viscosity increases due to reduction of cell-free region—formed due to shear-induced migration.^W For smaller diameter arteries ($d_1 \leq d \leq d_2$), the RBCs radially migrate toward the center of the artery and lead to a cell-free zone near wall, thus causing decrease in viscosity. When the diameter increases beyond micro-scale, this effect is not observed and hence viscosity reaches to a constant level with increased value. This is schematically shown in Fig. 3b where the zones of shear-induced migration are demarcated through values of d_1 and d_2 .

Other than the artery diameter, hematocrit, and shear rate, viscosity is also affected by physiological pulsatile flow behavior, health and complacency of artery, temperature of blood; however, these effects are much smaller. The various non-Newtonian models and their formulation are presented below. The elastic behavior of RBCs also lead to change in viscosity and is discussed separately. Finally, a CFD literature-based discussion on efficacy of various models is presented.

^W Under normal conditions, RBCs tend to align themselves in the center of blood vessels as they flow through. This phenomenon, known as the 'margination' or 'shear-induced migration' of RBCs, is a result of the shear forces within the blood vessel. The higher shear stress near the vessel walls encourages RBCs to migrate toward the center of the vessel, away from the slower-moving boundary layer near the walls.

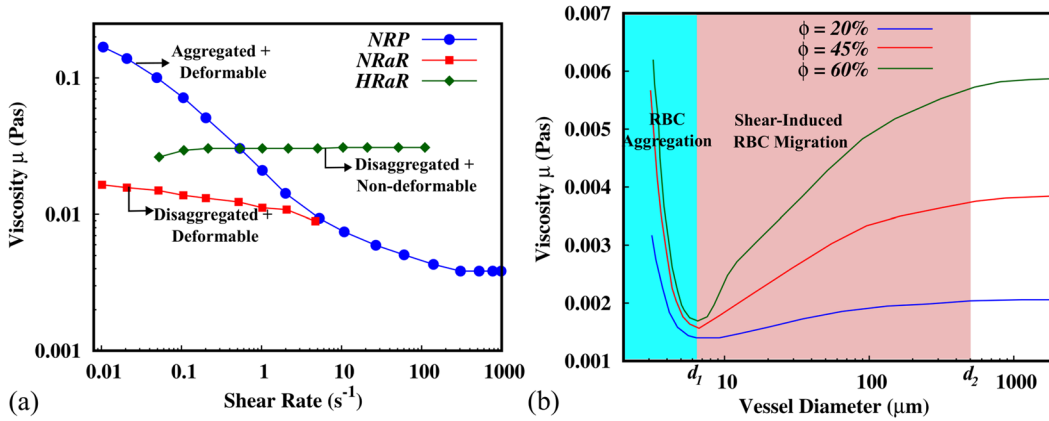


Figure 3: Variation of blood viscosity with **a** shear rate $\dot{\gamma}$ for three different types of plasma, and **b** vessel diameter for three different hematocrit levels ϕ of normal RBCs suspended in plasma (NRP) (obtained from data presented in Chien⁴⁷).

4.1 Non-Newtonian Models

Assuming the blood to be a continuum,^X the Newtonian model employs a constant/hematocrit level-based viscosity in the momentum conservation equation for hemodynamics (Eq. 2). In case of non-Newtonian models, the viscosity is a function of shear rate and/or hematocrit. The simplest non-Newtonian formulation is power law model, where an exponential curve is fit to the experimental data of viscosity variation with respect to (w.r.t.) shear rate $\dot{\gamma}$ given as

$$\mu = \mu_0(\dot{\gamma})^{n-1} \quad (13)$$

where $\mu_0 = 0.035 \text{ Pa s}^n$ and $n = 0.6$ ⁴⁷. A major disadvantage with this model is its inability to accurately predict viscosity at low and high shear rate. The model predicts unbounded viscosity at zero shear rate and zero viscosity when $\dot{\gamma} \rightarrow \infty$, which is unrealistic. Hence, several other non-Newtonian models were formulated using the $\dot{\gamma}$ and hematocrit ϕ , and the most commonly used models are summarized in Table 2. It can be observed that all the models use shear rate $\dot{\gamma}$ as input parameter in the definition while the Quemada model includes the RBC concentration ϕ along with shear rate. Apart from these shear-thinning models for viscosity, the thixotropic nature (time-dependent viscosity) of blood are modeled by several works^{48–50} but a generalized

power law (where the constant μ_0 depends on shear rate) is commonly used given as

$$\mu = \mu_0(\dot{\gamma})^{n_1} t^{n_2} \quad (14)$$

where the parameters μ_0 , n_1 , and n_2 are given in Braun and Rosen⁴⁹. Each of these models is evaluated against the Newtonian model-based CFD simulations in different arterial networks along with experiments, and the observations are presented in Sect. 4.3—to understand the significance/non-significance of non-Newtonian modeling.

4.2 Viscoelastic Behavior of Blood Constituents

In many situations, blood behaves as a viscoelastic fluid, i.e., it exhibits both viscous and elastic behavior. This unique property is crucial for its efficient flow through the intricate vascular network, and its ability to adapt to various physiological conditions. As it is generally understood and discussed in the above section, viscosity is related to the resistance of a fluid to relative velocity between the adjacent layers of the flowing fluid. In blood, viscosity arises primarily from the presence of plasma, a protein-rich fluid that surrounds the red blood cells. Plasma's viscosity contributes to the overall resistance to blood flow, particularly in narrow capillaries. Elasticity, on the other hand, describes a material's ability to store and release energy upon deformation. In blood, RBCs play the primary role in imparting elasticity. These cells, being flexible and deformable, can temporarily change shape to navigate through narrow capillaries (when shear rate is low) and return to their original shape as they

^X Conceptual model used in fluid mechanics that treats a fluid as a continuous substance without any gaps or discontinuities at the microscopic level. It's based on the idea that within a fluid, the properties, such as velocity, pressure, density, and temperature, vary continuously throughout space and time.

Table 2: Summary of commonly used non-Newtonian models for modeling hemodynamics.

Model	Expression for μ	Parameters
Modified power-law ⁵¹	$C_1 \exp(C_2 H_t) \dot{\gamma}^{-C_3 H_t}$	$C_1, C_2,$ and C_3 —experimentally determined, $H_t \approx 0.4$
Carreau ⁵²	$\mu_\infty + (\mu_0 - \mu_\infty)[1 + (\lambda \dot{\gamma})^2]^{(n-1)/2}$	$\mu_0 = 0.056, \mu_\infty = 0.00345$ $n = 0.3568, \lambda = 3.31 \text{ s}$
Carreau and Yasuda ⁵²	$\mu_\infty + (\mu_0 - \mu_\infty)[1 + (\lambda \dot{\gamma})^q]^{(n-1)/q}$	$\lambda = 1.9 \text{ s}, n = 0.22, q = 1.25$
Cross ¹⁶	$\mu_\infty + \frac{(\mu_0 - \mu_\infty)}{1 + (\lambda \dot{\gamma})^m}$	$\lambda = 1.007 \text{ s}, m = 1.028$
Casson ⁵³	$[\sqrt{\mu_c} + \sqrt{\tau_c/\dot{\gamma}}]^2$	$\mu_c = 0.0042 \text{ Pa s}, \tau_c = 0.0038 \text{ Pa}$
Quemada ⁵⁴	$\mu_0 \left[1 - \frac{\phi}{2} \frac{k_0 + k_\infty \sqrt{\dot{\gamma}/\dot{\gamma}_c}}{1 + \sqrt{\dot{\gamma}/\dot{\gamma}_c}} \right]^{-2}$	$\mu_0 = 0.0012 \text{ Pa s}, \dot{\gamma}_c = 1.88 \text{ s}^{-1}$ $k_0 = 4.33, k_\infty = 2.07, \phi = 0.4$

exit. This elastic behavior allows blood to flow smoothly through small vessels without significant energy loss. The viscoelastic nature was first discussed in the works of Thurston et al.⁵⁵. Later, for simulating viscoelastic blood, several other works were performed^{56,57} to come up with suitable mathematical model.

Although viscoelastic nature of blood leads to modeling complexity, it is particularly important in several physiological situations; like discussed here for four such situations. First, for microcirculation in tiny capillaries (where red blood cells are tightly packed), blood elasticity enables them to deform and squeeze through these narrow passages, ensuring efficient delivery of oxygen and nutrients to tissues. Second, for hemodynamics, the elastic recoil of RBCs contributes to the pulsatile flow of blood—helping to maintain blood pressure and facilitate blood movement. Third, blood filtration in the kidneys, where elasticity of RBCs allows them to pass through the glomerular filtration barrier while retaining larger molecules like proteins; and fourth, blood coagulation during blood clot formation, where the elasticity of RBCs helps to concentrate clotting factors and promote clot formation at the site of injury.

After introduction of the viscoelasticity concept for blood by Thurston⁵⁵, Oldroyd⁵⁶ gave an empirical model to evaluate stress tensor—by fitting the experimental curves with proposed model. This model effectively represents how blood's viscosity decreases with increasing shear rates—known as shear-thinning behavior—along with the elasticity of blood particles. However, it fell short as it did not account for variation of

relaxation times^Y with shear rates that contradicted the experimental findings. The model devised by Anand and Rajagopal⁵⁷, within the general thermodynamic framework outlined in Rajagopal and Srinivasa⁵⁸, incorporates variation of relaxation times with the shear rate. This formulation yields favorable conformity with empirical observations in both steady Poiseuille and oscillatory flow scenarios. In general, the deviatoric stress tensor $\bar{\tau}$ (Eq. 2) can be modeled as a combination of viscous ($\bar{\tau}_s$) and elastic ($\bar{\tau}_e$) stress, i.e., $\bar{\tau} = \bar{\tau}_s + \bar{\tau}_e$, where

$$\bar{\tau}_s = \mu(\dot{\gamma}) \left(\nabla \vec{u} + (\nabla \vec{u})^T \right) \quad (15)$$

and $\bar{\tau}_e$ satisfies Oldroyd-B type constitutive equation, given as

$$\begin{aligned} \frac{\partial \bar{\tau}_e}{\partial t} + (\vec{u} \cdot \nabla) \bar{\tau}_e &= \frac{2\mu_e}{\lambda_1} \bar{D} - \frac{1}{\lambda_1} \bar{\tau}_e + (\bar{W} \bar{\tau}_e - \bar{\tau}_e \bar{W}) \\ &+ (\bar{D} \bar{\tau}_e + \bar{\tau}_e \bar{D}) \end{aligned} \quad (16)$$

where \bar{D} and \bar{W} are symmetric and anti-symmetric part of velocity gradients, μ_e is the elastic viscosity co-efficient, and λ_1 is the relaxation time ($\approx 0.06\text{s}$). The above equation is solved along with standard mass and momentum conservation laws to obtain the complete viscoelastic response of blood. Many authors have performed such investigations, but mostly in a single phase setting. Apart from the above presented visco-elastic models, the most accurate method would be to actually introduce RBCs in blood and model their

^Y relaxation time refers to the characteristic time it takes for the blood to return to its resting state or original configuration after experiencing a disturbance or change in flow conditions.

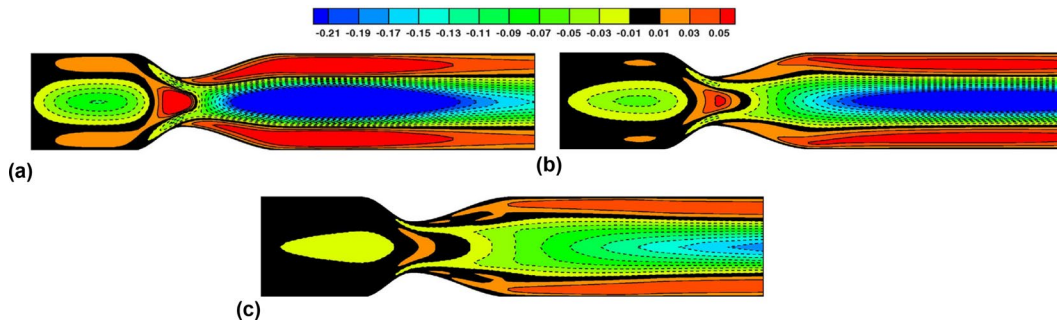


Figure 4: For steady flow in axisymmetrically stenosed artery, contour map of normalized difference between the solutions of generalized Oldroyd-B and Newtonian models with flow rate **a** $Q = 0.5 \text{ cm}^3/\text{s}$, **b** $Q = 1 \text{ cm}^3/\text{s}$, and **c** $Q = 2 \text{ cm}^3/\text{s}$ (Figure adapted from Bodnar et al.⁶² with permission from Elsevier).

deformation dynamics numerically. RBCs continuously change the shape depending on shear rates in the stream and can be simulated using the models presented in Hoque et al.^{59,60} and Fedosov et al.⁶¹ etc., especially for micro-vessels. However, it should be noted that these simulations encounter a large variation in the scale (μm to cm) and can be difficult to model computationally—due to high computational cost and stability issues. In order to access whether such involved modeling is necessary or not, a brief survey of literature for such comparisons and major observations presented are discussed below.

Bodner et al.⁶² performed a comparative CFD study between Newtonian, simplified non-Newtonian (without elastic stress), and generalized Oldroyd-B model, by performing blood flow simulations in axisymmetric stenosed artery and patient-specific carotid bifurcation. It was reported that blood flow in medium-sized blood vessels exhibits shear-thinning and viscoelastic behavior, and these non-Newtonian effects were influenced by low flow rate. This was proved by comparing normalized difference between the solutions of Newtonian and generalized Oldroyd-B model, as shown in Fig. 4. A similar study⁶³ discussed the effects of shear-thinning and viscoelastic properties on blood flow in abdominal aortic aneurysms, under different flow rates. Their results showed that the blood shear-thinning behavior and viscoelasticity cannot be neglected especially for low shear rates conditions. Further, Chen et al.⁶⁴ studied the effects of hematocrit, plasma concentration, and frequency of sinusoidal oscillatory shear flow on the viscoelasticity of human blood. They also demonstrated that the viscous and elastic component increased exponentially at higher hematocrit levels; and exponential decrease in viscous and elastic components of blood with increased frequency of

shear flow. Thus, from the above studies, it can be concluded that the viscoelastic non-Newtonian modeling is necessary for blood flow in (a) low/medium size vessels ($d \leq 2 \text{ mm}$), (b) low flow rate condition, and (c) low Womersley (Wo) number.^Z

4.3 CFD-Based Comparison of Viscosity Models

The above sub-sections presented various non-Newtonian models for hemodynamic analysis. Since implementation of these schemes comes with increased modeling complexity and computational cost, it is important to understand whether they are necessary for artery and flow conditions under consideration. Thus, a CFD-based comparison of such models with Newtonian counterpart is presented here. Neofytou⁶⁵ performed two-dimensional CFD simulation on an indented (constricted) channel with moving top wall (where indentation is present). The wall moved with two different time-periods (Strouhal number^{AA} St): 0.05 and 0.368, and four different viscosity models were used: (a) Newtonian, (b) power law, (c) Casson, and (d) Quemada. For a constant inlet velocity, the author observed that non-Newtonian effects are more clearly visible for $St = 0.05$. Also, the maximum and minimum WSS values are underpredicted with Newtonian

^Z The Womersley number (Wo) is a dimensionless number used in fluid dynamics to characterize the unsteadiness of pulsatile flow, particularly in blood flow analysis. It is a dimensionless expression of the pulsatile flow frequency in relation to viscous effects. It is calculated as $Wo = R\sqrt{\omega/\nu}$, where R is radius of artery, ω is angular frequency of pulsation, and ν is kinematic viscosity of fluid.

^{AA} A non-dimensional frequency parameter given by $St = fD/u$, where f is frequency of flow pulsation (Hz), D is arterial Diameter, and u is characteristic flow velocity.

and power law viscosity model, whereas Casson and Quemada models give similar values of WSS for both values of St . Thus, for flexible walls with lower elasticity, the author concluded that it is important to consider a good non-Newtonian viscosity model to predict the hemodynamics accurately.

Apart from the two-dimensional model, for rigid model of CCA, Razavi et al.⁶⁶ performed axisymmetric^{AB} CFD simulations with four different stenosis levels and seven different viscosity models: Newtonian, power law, generalized power law, Casson, Carreau, Carreau–Yasuda, and Walburn–Schneck models. A pulsatile flow based on physiological conditions was used at the inlet of artery. Along with hemodynamic parameters, they defined a parameter, termed as global non-Newtonian Importance Factor (*NNIF*), and was calculated at different time instants of cardiac cycle. They observed a deviation from Newtonian behavior during lower velocity, i.e., during diastolic phase.^{AC} Further, they observed that the non-Newtonian behavior is over-estimated by the power law model while under-estimation by generalized power law and Casson models. The Carreau and Carreau–Yasuda model gave moderate *NNIF* values during lower shear rates only, and hence were suggested to be better models. For hemodynamic parameters WSS and OSI, they found almost same results from all the models except power law and Casson model; indicating Newtonian behavior of blood at most of the time instants.

In order to understand whether non-Newtonian model is really necessary for large arteries, Arzani⁶⁷ performed a CFD investigation on patient-specific carotid-artery aneurysm using Newtonian, Carreau–Yasuda and a novel hybrid viscosity model. The novel model was developed, using Lagrangian tracking-based Residence Time (RT) of RBCs in aneurysm sacs. The author argued that apart from lower shear rate ($<50 \text{ s}^{-1}$), the amount of time spent by RBCs in recirculation zone also matters since rouleaux formation and RBC aggregation takes around 5–10 s. The main motivation behind author's argument was

the observation made in rheology experiments, where shear-thinning behavior was observed after some time—when shear rate went below threshold. This was attributed to the reason that some time is required for RBC to aggregate and increase the effective viscosity. Hence, if the $RT > RT_{th}$ (either 5 or 10 s), the non-Newtonian model is activated. The results obtained for pulsatile blood flow in aneurysm sac indicate that the non-Newtonian behavior is *rarely achieved* for large arteries (like carotid). Further, the hemodynamic indicators like WSS, time-averaged WSS (TAWSS), and OSI remain almost same, between the Newtonian and proposed hybrid non-Newtonian model, since the RT remains below 5 s for most of the locations during pulsatile cardiac cycle.

Most of the studies on viscosity models involved CFD (discussed above), while the in vitro measurements were missing. Recently, for effect on different viscosity models on the hemodynamics of patient-specific left anterior descending (*LAD*) coronary, Abbasian et al.⁶⁸ performed a systematic investigation using CFD, and compared their results with 4D MRI. The arterial mid-point flow velocity, obtained using 16 different viscosity models, for three atherosclerotic patient arteries were compared with clinical measurements using 4D MRI. They observed that Newtonian model provides accurate results in the proximal region of atherosclerosis while the Casson, Carreau–Yasuda, and Quemada model compare better, with the clinically measured velocities, in the distal region. Further, the time-averaged hemodynamic parameter, calculated using Newtonian model, compared well with those calculated using Casson, Carreau–Yasuda, and Quemada model, whereas the instantaneous hemodynamic parameters like WSS, OSI varied significantly for Newtonian model. Thus, the clinical measurements were used as benchmark to understand which viscosity model is best suitable for performing CFD study in coronary arteries—most susceptible to plaque deposition.

For understanding the limitations of non-Newtonian models and their deviations from Newtonian counterparts, Karimi et al.⁶⁹ performed a CFD study on patient-specific geometry of *aortic arch*, obtained using CT scan, for nine different viscosity models for blood. The artery is modeled as rigid and an idealized transient inflow velocity, with zero-gage pressure at outlets, is specified. The *NNIF* is obtained by measuring the difference between WSS of various non-Newtonian models with a Newtonian model (constant viscosity $\mu = 0.0035 \text{ Pas}$). It is observed that the

^{AB} Axisymmetric simulations are a type of computational modeling used to study fluid flow around bodies that possess axial symmetry. In these simulations, instead of modeling an entire 3D domain, a 2D cross section is employed and rotated around an axis to represent the complete geometry.

^{AC} This phase occurs when the heart relaxes. The left ventricle relaxes and refills with blood from the atria. Blood continues to flow through the arteries, but the pressure and velocity are lower compared to systole (heart contraction)

Table 3: Summary of literature on various CFD-based viscosity models and their outcomes.

Author	Artery studied	Viscosity model and other physics studied	Observations
Neofytou ⁶⁵	2D channel with coronary dimensions	Newtonian, power law, Casson and Quemada, on moving artery wall	Casson and Quemada—similar values. non-Newtonian behavior at lower frequencies only
Razavi et al. ⁶⁶	Stenosed carotid artery (axisymmetric)	Seven different viscosity models, including power law, Casson, Carreau–Yasuda	Similar hemodynamics with Newtonian models. Carreau and CY model—moderate instantaneous differences
Arzani ⁶⁷	Intracranial aneurysm	Hybrid non-Newtonian (using CY) when $RT_{RBC} > 5$ s (using Lagrangian RBC tracking)	Hemodynamics similar to that of Newtonian during most time instants
Abbasian et al. ⁶⁸	Stenosed LAD coronary	16 different viscosity models (comparison with 4D MRI)	Proximal (distal) of stenosis—good comparison with Newtonian (CY, Quemada)
Karimi et al. ⁶⁹	Aortic arch	Nine different viscosity models (comparison with Newtonian CFD)	Deviation of cross model highest—not suitable to use

cross model has largest deviation from Newtonian model while the other viscosity models yield closer results with Newtonian models. It is suggested by the authors that since these models are developed by a curve fitting procedure on experimental data obtained from steady flow cases, it is better to avoid cross type-of-models where deviations are high. Instead, the Carreau and generalized power law, which consider Newtonian viscosity at high shear rates, are more realistic, especially in large arteries where the flow is Newtonian in most of the flow domain.

Finally, Yilmaz et al.⁷⁰ provided a review of various rheological models, proposed for modeling blood in *human vasculature*. The authors discuss about the composition of blood; and critically review the commonly used (in CFD) viscosity models (Newtonian and non-Newtonian), thixotropic properties, and elastic models (Olroyd-B, yield stress formulation). They highlight main issues and future scope, including (1) dependence of critical shear rate for disaggregation of RBC on the hematocrit level, (2) dependence of viscosity on pulsatile flow period and setup, (3) inability to measure threshold time for occurrence of aggregation so that non-Newtonian behavior is predicted accurately, and (4) measurement of thixotropic properties of blood. A summary of all the above discussed literature is presented in Table 3. The table shows that, for large arteries (carotid, aorta) involving transient flow, the non-Newtonian behavior is diminished while the blood-flow strongly deviates from constant viscosity for small arteries ($d < 2$ mm). Further, Quemada and Carreau–Yasuda

model are found to be best suited for non-Newtonian modeling while power law and its derived models are found to have abnormal deviation in hemodynamics.

5 Role of Fluid–Structure Interaction in Computational Hemodynamics for Complaint Vasculature

Computational fluid–structure interaction (CFSI) is a multi-physics problem which involves deformation of solid due to fluid forcing and simultaneous change in region of fluid flow due to solid movement. Blood moves out of aorta with a high pressure since it has to be transported to other regions of body while it comes back from capillary and veins with lower pressure. During the systolic phase (high flow rate), high blood pressure experiencing artery expands and later contracts elastically to serve two purposes: (a) lower the sudden impact of high pressure load on the artery wall and (b) store some amount of blood (by expanding) so that during diastolic phase (very low flow rate), this additional blood may be supplied to organs by gradual contraction so as to avoid oxygen deprivation in the organs. Thus, it can be observed that FSI modeling in elastic arteries becomes essential to capture the hemodynamics accurately. From the prediction of aneurysm rupture to calculation of correct blood flow rate in aortic dissection, elastic wall modeling has been observed to yield more accurate outcomes (in comparison with in vivo measurements) discussed in the next subsections.

CFSI involves coupled solutions to Navier–Stokes equations (through computational fluid dynamics—CFD) and structural momentum conservation laws (through computational structure dynamics—CSD). As discussed in a recent review article on CFSI methodologies and applications by Morab and Sharma⁷¹, there have been numerous works^{72–74} in the area of development of CFSI algorithms and solvers. All these numerical works are classified based on the way coupling between fluid and solid is achieved, and also on the way in which the grid is generated and gets deformed. FSI can be modeled using a monolithic or partitioned approaches. The monolithic approach involves formulating a single equation for fluid and structure⁷⁵; however, these methods are limited to linear deformation problems and need to be modified or changed completely for different problems, whereas the partitioned approach involves separate equations that lead to a coupled solution of the existing fluid and solid solvers discussed by Hughes et al.⁷⁶ and Trepanier et al.⁷⁷, using the finite element (FE) and finite volume (FV) discretization methods, respectively. Further, a classification based on the type of mesh generated to solve fluid solid interactions leads us to body conforming and non-conforming type mesh (Fig. 5). In case of body conforming type system⁷⁸, the interface between fluid and solid is considered to be a physical boundary. In most of the cases, fluid particles are tracked through Eulerian approach whereas solid movement is tracked via Lagrangian formulation, and the mesh is regenerated and/or deformed as per solid deformation. In case of non-conforming mesh methods^{79,80}, the interface conditions are not treated as physical boundary conditions for fluid and solid domain. They are treated in governing equations itself so as to give the same effect of boundary conditions (no slip and specified traction). The major advantage with these methods is that, though fluid and solid are discretized quite differently, a static initial mesh is used for an FSI problem; thus, re-meshing is not needed that reduces the computational cost. Efficient mathematical formulation of governing equation for accurate interface conditions needs to be considered.

From the above discussion, it can be noticed that there are many techniques, which have different time complexities,^{AD} to model interaction

^{AD} Time complexity refers to the computational efficiency of an algorithm, representing how the execution time of the algorithm grows concerning the input size. It helps in understanding how an algorithm's performance scales as the size of the input increases.

of blood flowing through lumen^{AE} with elastic artery wall. It becomes important to first understand whether modeling vessel wall deformation is really necessary or not, and second, choose the optimum method so that accurate results with minimum computational time are obtained. Thus, a detailed literature survey for different computational techniques and their outcomes is presented in a separate subsection below.

5.1 Studies on Computational Hemodynamics with FSI

Hirschhorn et al.⁸² provided a comprehensive review of various FSI works performed for Cardiovascular flows. They presented various methodologies to model the multi-physics problem of arterial deformation and blood flow. They reported that the immersed boundary method (IBM), which can handle large deformation, is gaining popularity with improvement in computational power. Further, a review of FSI models applied to understand blood-flow in vascular aneurysms, cardiac valves, prosthetic valves, atherosclerosis regions, and stented artery was detailed along with relevant literature between 2017 to 2019.

Blood flow in compliant/flexible aortic dissection was numerically modeled using two-phase (RBC suspended in plasma) non-Newtonian model (Carreau–Yasuda) by Qiao et al.²⁴. The mixture model for two-phase flow, along with empirical models for shear lift force and interface momentum exchange was employed for spherical RBC particles suspended uniformly in plasma at the inlet. arbitrary Lagrangian Eulerian (ALE) method was employed for FSI modeling, with artery (structure) modeled as linear isotropic material. From the multi-physics simulations, it was observed that, although TAWSS did not vary much between single, multiphase, and rigid models, OSI varied significantly between single and multiphase non-Newtonian models while a small difference with rigid model was observed. Overall, the authors concluded that consideration of multi-phase model can alter the hemodynamics and lead to different conclusion on the pathogenesis of atherosclerosis. Further, in order to understand the effect of arterial elasticity and blood visco-elasticity, Bilgi and Atalik⁸³ performed FSI simulation with Newtonian and non-Newtonian Oldroyd-B model. They reported that von-Mises stresses on arterial wall increase with

^{AE} The lumen of an artery is the hollow space inside the vessel through which blood flows.

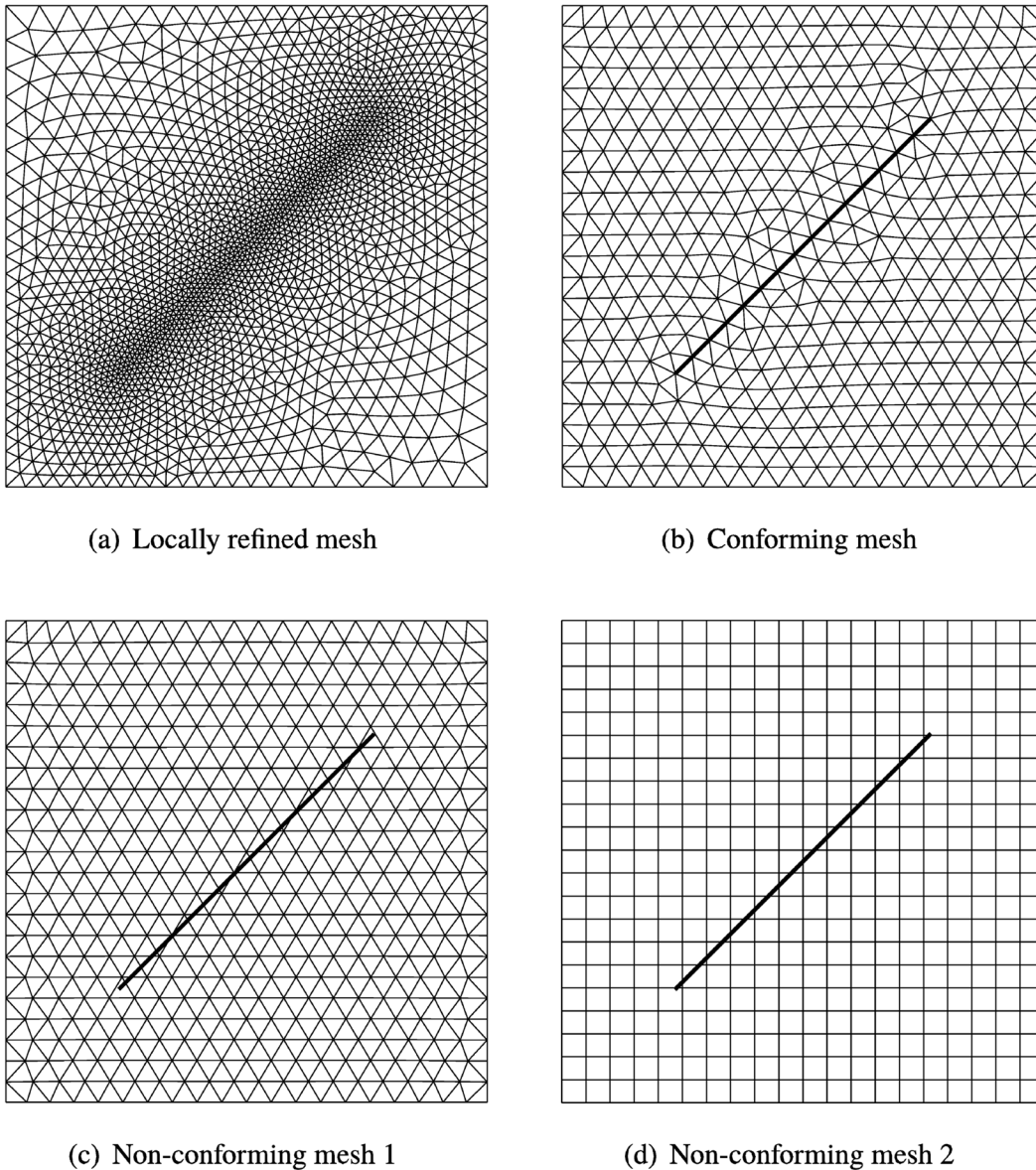


Figure 5: Illustration of various meshing techniques employed in CFSI problems (Adapted from Xu and Yang⁸¹ with permission from Elsevier).

fluid's elasticity and hence may increase in arterial deformations. This study was performed for aneurysm; however, no such study was found for stenosis.

In order to improve the accuracy of computational results, Baumler et al.⁸⁴ performed a two-way coupled FSI simulation on pre-stressed aortic arch^{AF} with true and false lumen separated by flexible aortic dissection. The main motivation of the work was to come up with an accurate model,

^{AF} A curved structure that arises from the ascending aorta (artery coming out from heart), takes a sweeping arch-like shape, and then descends through the thorax.

which could predict flow velocity and deformations in aorta so that the hemodynamics, after a surgery, can be predicted well using the CT scan geometry. The pre-stressing of artery was performed to adjust the CT scan-based geometry with the diastolic load which is present during image capture. Further, a non-linear hyper-elastic model for aortic dissection and artery wall, with elastic modulus varying from 20 to 800 kPa, was considered for simulation. A comparison of velocity and deformation results with 4D MRI measurements (in vivo) showed that the optimized numerical model was able to capture maximum deformations and systolic velocities

with a good accuracy, which were underpredicted by non-pre-stressed and untethered numerical simulations.^{AG} The results of FSI model showed low TAWSS values in false lumen regions, thus making them prone to endothelium degeneration. Further, the false lumen flow rate was observed to decrease with increasing elastic modulus, indicating pathogenesis for atherosclerosis.

It is important to understand whether a complete FSI simulation or a standalone CFD and/or CSD simulations are sufficient to predict artery rupture in aneurysms. This would lead to reduction of computational cost, which is extremely necessary in a clinical setup. In order to gauge this, Valencia et al.⁸⁵ performed a comparative hemodynamic study on patient-specific cerebral aneurysm geometry using coupled FSI (with a constant elasticity for artery), purely CFD, and purely CSD (with different elastic models) studies. Their CSD model considered segment of aneurysm and complete aneurysm model as two cases with multiple elastic models like hyper-elastic, Mooney–Rivlin, modified MR with experimental data, etc. They observed that CSD and CFD simulations underpredicted the effective stress values as compared to the coupled FSI simulations. Further, there were changes in hemodynamic parameters along with effective stress values for CSD model—with constant elasticity and various non-linear material models. These deviations were minor as compared to a 63% increase in stress observed for a hypertensive artery. Thus, the authors highlighted that the use of FSI simulations with non-linear material modeling can yield similar results as compared to a simpler model for normal physiological loads, but consideration of proper pressure boundary condition (like Windkessel^{AH} model) is highly essential.

In order to understand the role of arterial elasticity on low-density lipoprotein (LDL) uptake in left coronary artery (LCA), Chen et al.²⁵ performed FSI simulations on a patient-specific LCA geometry with four cases involving rigid artery, flexible artery with different thickness, and two different blood pressure levels. It was reported

that the elastic nature of artery introduced complex flow patterns which reduced the LDL accumulation. Thus, consideration of rigid models can lead to over-prediction of LDL prediction and lead to unnecessary medical treatments. Further, the authors also reported that hypertension (modeled using high blood pressure) can lead to larger changes in LDL accumulation, as compared to that in the rigid versus compliant model.

Chiastra et al.⁸⁶ investigated the importance of considering flexible nature of artery while computing hemodynamic factors in a stented coronary artery, to monitor a patient for post-surgery complications. Using a commercial software ADINA, they performed two-way coupled FSI simulations for *coronary artery* with two different stent materials. Further, the results were compared with same geometries modeled as rigid (without deformations). They found that, for idealized models of a stented coronary artery, the rigid wall assumption for fluid dynamic simulations appears adequate when the aim of the study is the analysis of near-wall quantities like WSS. The authors compared the results of fluid–structure interaction (FSI) and corresponding rigid wall models, focusing on the analysis of the WSS distribution. They found that the trends in terms of instantaneous and time-averaged WSS were similar—between compliant and rigid wall cases. Further, between the FSI and the rigid wall cases, the difference of percentage area exposed to TAWSS < 0.4 Pa was about 1.5% for cobalt–chromium (CoCr) and 1.0% for poly-L-lactide (PLLA) stents.

In order to understand the effect of arterial flexibility and RBC movement on the resulting hemodynamics for multiple stenosed coronary arteries, Athani et al.⁸⁷ performed multi-phase FSI simulations on patient-specific Left Coronary Artery (LCA). The fluid domain was solved, using a finite volume-based commercial software (Fluent R2020), with multi-phase modeling performed using the mixture model. The fluid (blood) and the solid (wall) domains were fully coupled using the ANSYS FSI solver. They evaluated hemodynamic parameters, such as WSS, pressure, velocity, in the patient's left coronary artery while considering the walls to be rigid and flexible. They found overestimation of hemodynamic descriptors for the rigid models as compared to the FSI models. The region of larger displacement occurs at the pre-stenosis area as compared to the other area of the left coronary artery model. They observed an increase in blood flow velocity across the restricted regions

^{AG} Tethered numerical simulations in fluid–structure interaction (FSI) involve modeling the interaction between fluids and structures, where one or more solid structures are connected to the fluid domain by tethers or cables. This is implemented by giving Dirichlet boundary condition for deformation at least one end.

^{AH} A windkessel, which translates to “air chamber” in German, is a component in various systems that acts as a reservoir to dampen pressure fluctuations and ensure a smoother flow of fluid.

(stenosis) in the LCA, and the recirculation zone at the post-stenosis and bifurcation regions was noted.

5.2 Linear and Non-linear Material Model for Artery

From the extensive review of CFSI modeling methods for blood flow, it is understood that blood flow patterns, accumulation of blood particles and hemodynamic parameters change significantly due to arterial deformations. Hence, consideration of FSI is necessary for both conducting^{AI} and distributing^{AJ} vessels. Apart from selection of suitable FSI and rheological model for blood, it is also very important to model the artery wall deformation accurately. As discussed in Sect. 2, the constitutive relation between σ and ϵ are different for linear and non-linear material models. A brief description of these material models is presented in Table 4. For the commonly used linear material model, the stress is related linearly with strain using elasticity matrix [D], which can be calculated using Hooke's law for plain-strain/stress cases. For non-linear artery model, the stress tensor is defined in terms of derivative of strain–energy function W , which is a non-linear function of strain field E . Although non-linear material models are found to be more realistic and provide closer results with in vivo observations, the associated modeling is mathematically challenging and computationally very expensive. Also, it is reported in the literature that, as we move away from heart, the arteries become thick and have lesser deformation—due to which linear models can be valid. Hence, a brief literature survey of effect of different artery wall model on resulting deformation accuracy is presented below, which enables selection of an appropriate model that is suitable for the artery under investigation.

For artery wall modeling, nonlinear and linear models have been compared in several studies. The choice between these models depends on factors, such as accuracy, ease of implementation, and computational costs. Nama et al.⁹⁴ presented a systematic comparison between linear and non-linear artery wall modeling approaches, including membrane, shell, and 3D solid formulations. The comparison is presented in an idealized bifurcation model for regionally varying wall thickness, while incorporating the effect of external tissue surrounding the vessel wall. It was reported by authors that although membrane model gave comparable results with available axisymmetric

solutions, they failed to converge for bifurcation geometries. Shell models with linear elastic model, which have fewer degrees of freedom, yield closer results with 3D solid model (P2 wedge-type) and hence can be considered optimal for simulation of artery wall response.

Solovyova et al.⁹⁵ compared the use of the linear and nonlinear models, for artery wall modeling, in the context of blood flow and pulse wave propagation. They presented a brief review of the nonlinear models, and applied both 2D linearized and 1D nonlinear models in their study. They reported that nonlinear models better describe degenerated pathological walls while linear models satisfactorily describe healthy elastic walls. On a contrary note, Baier et al.⁹⁶ linearized the general non-linear elastic model and compared the displacements with those obtained nonlinear model. Authors reported that linear model matches well with nonlinear model in normal physiological conditions while intima layer^{AK} shows deviation in large deformation cases (abnormal physiological loads). Oshima and Tori⁹⁷ performed FSI simulations, for blood flow in patient-specific aneurysm with linear and general non-linear model for artery wall deformations. Their comparison between artery wall model showed that linear model over-predicts the wall stresses and can lead to high rupture-risk prediction. From the above literature survey, it can be observed that linear models can be considered in healthy artery (with normal physiological loads) while they might lead to lower deformations in highly calcified arteries and those with aneurysms. Regarding choice of suitable non-linear artery model, there is no single consensus and is generally suggested that specific artery parameters may be considered—in the constitutive relation of a general non-linear artery model.

6 Concluding Remarks and Future Outlook

Understanding the complexities of blood-flow dynamics within the human vasculature is important for understanding numerous physiological and pathological phenomena. In this comprehensive review, we present computational fluid dynamics (CFD) modeling techniques applied to blood flow, aiming to address crucial questions shaping the contemporary research. Our investigation centers on three critical decisions one has to

^{AI} vessels carrying blood from heart to other arteries.

^{AJ} vessels carrying blood from main artery to arterioles and capillaries.

^{AK} The intima is the innermost layer of an artery. It is composed of endothelial cells that line the interior surface of the blood vessel.

Table 4: Summary of most commonly used material models for FSI modeling in vasculature.

Model	Definition	Parameters
Linear elastic	$[\sigma] = [D] [\epsilon]$	$[D]$ —elasticity matrix, $[\epsilon]$ —strain matrix
General non-linear elastic ⁸⁸	$[\sigma] = [F] \frac{dW}{dE} [F]^T, E = 0.5([\mathbf{F}][\mathbf{F}]^T - \mathbf{I})$	W —strain-energy function, $[F]$ —deformation gradient tensor
Hyper-elastic ⁸⁹	$W = \sum_{i=1}^3 A_i E_{ii} + \sum_{i=1}^3 \sum_{j=1, j \neq i}^3 A_{ij} E_{ij}^2 + 0.5\kappa(I_3 - 1) + O(E^3)$	A_i, A_{ij}, κ —material parameters determined from experiments
Fung and Chuong ⁹⁰	$W = 0.5c(e^Q - 1);$ $Q = c_1 E_{RR}^2 + c_2 E_{\theta\theta}^2 + c_3 E_{ZZ}^2 + 2c_4 E_{RR} E_{\theta\theta} + 2c_5 E_{\theta\theta} E_{ZZ} + 2c_6 E_{ZZ} E_{RR}$	c_j —dimensionless material constants
Modified Mooney–Rivlin model ⁹¹	$W = C_1(I_1 - 3) + C_2(I_2 - 3) + C_3(I_1 - 3)^2 + C_4(I_1 - 3)(I_2 - 3) + C_5(I_2 - 3)^2 + C_6(I_1 - 3)^3 + C_7(I_1 - 3)^2(I_2 - 3) + C_8(I_1 - 3)(I_2 - 3)^2 + C_9(I_2 - 3)^3 + D_1(e^{D_2(I_1 - 3)} - 1)$	C_i and D_1 —constants with stress dimensions, D_2 —dimensionless material parameter, I —invariant of Cauchy–Green tensor
Odzen hyper-elastic ⁹²	$W = \sum_{i=1}^3 \frac{2\mu_i}{\alpha_i^2} (\lambda_i^{\alpha_i} + \lambda_2^{\alpha_i} + \lambda_3^{\alpha_i} - 3) + \sum_{i=1}^3 \frac{1}{D} (J - 1)^{2i}$	J —volumetric stretch, λ_i —stretches in the principal directions
Incompressible polynomial ⁹³	$W = \sum_{i=1}^6 C_{i0}(I_1 - 3)^i$	$C_{10} - C_{60}$ —polynomial model parameters (vary with artery)

make while modeling hemodynamics in human vasculature. First, the relevance of non-Newtonian models in varying vascular conditions and the alterations required to incorporate the viscoelastic nature of red blood cells (RBCs). Second, the validity of single-phase assumptions versus multiphase modeling, particularly concerning arterial geometries and potential particle migration effects; and third, the impact of arterial wall elasticity on blood flow patterns—in order to understand whether a rigid wall assumption suffices or a fluid–structure interaction (FSI) model is required.

Based on an extensive survey of literature encompassing diverse scenarios in blood flow modeling within human vasculature, several key insights have emerged. First, the significance of non-Newtonian blood behavior becomes pronounced in specific conditions: notably, severely stenosed arteries fostering recirculation zones or those with diameters below 4 mm and low Womersley numbers Wo . In these cases, viscoelastic models exhibit substantial deviations from simple Newtonian models, surpassing a 10% difference in predicted outcomes. Conversely, larger arteries like the carotid and aorta, experiencing highly pulsatile flows with elevated Wo , maintain characteristics similar to Newtonian fluids. Secondly, the debate between single-phase and multiphase modeling reveals subtle differences. While straight arteries with stenosis or aneurysms show

minimal distinction between these approaches, curved and branched arteries showcase noteworthy particle migration effect that influences hemodynamic parameters. Interestingly, single-phase equations, when integrated with the Philips diffusive flux model, yield promising results as compared to two-phase models; especially in certain arterial configurations. Lastly, the role of arterial wall elasticity manifests differently across various scenarios. Complaint arterial models, as compared to rigid models in larger arteries or those lacking elastin, maintain similar hemodynamics. However, instances, such as hypertension and simulations of blood-flow in smaller arteries, underscore the significance of fluid–structure interaction (FSI) in altering hemodynamic patterns. Based on the literature survey, a brief summary of appropriate physiological modeling techniques is presented in Table 5.

In conclusion, the choice of modeling approach for blood flow in human vasculature must be judiciously tailored to the specific vascular scenario under consideration. Non-Newtonian modeling gains prominence in narrower or more pathological vessels, while the choice between single-phase and multiphase modeling hinges on the vascular geometry and potential particle migration effects. Furthermore, the influence of arterial wall elasticity, particularly in diseased states, underscores the relevance of FSI in accurately

Table 5: Summary of literature review on suitable modeling techniques, which can be employed for physiological simulations in different arterial network.

Artery network ($Re_{max,D}$)	Multiphase model (required or not?)	Suitable rheological model for blood	Arterial complacency (any significant effect?)
Abdominal (1400, 16 mm)	Less critical in arteries with high flow rates. Primarily affects flow patterns and turbulence in complex bifurcations	Newtonian model and Cross model for viscoelasticity if considering vessel compliance	Minor impact on pressure and flow, moderate impact on flow patterns
Femoral (1100, 8 mm)	Not crucial for pulsatile flow, but helpful for steady and aneurysms. Minor impact on pressure and flow, and WSS	Quemada model for shear thinning	Can be neglected in healthy vessels, potentially significant in aneurysms or complex geometries
Carotid (1000, 6.2 mm)	Not necessarily required for large arteries unless gas bubbles are present. May affect WSS in smaller branches	Newtonian model (pulsatile flow)	Can be neglected, small impact on pressure and flow
Intracranial (700, 4.5 mm)	Important for assessing hemodynamic risks like aneurysms and vasospasm. Can significantly influence pressure and flow distribution in small, tortuous vessels	Carreau–Yasuda with additional factors for Fahreus–Lindqvist effect (cell aggregation)	Significant impact on WSS, pressure gradients, and flow patterns
Coronary (200, 4 mm)	Important for capturing non-uniform blood flow with cell-cell interactions, especially in curved geometries	Carreau–Yasuda for shear thinning and Oldroyd-B for viscoelasticity	Significant impact on WSS, pressure, and flow, especially in diseased vessels

simulating hemodynamics, thus showing the multifaceted nature of blood-flow modeling within the human vasculature. Although significant progress has been made in computational modeling, clinical implementation of such studies have been rarely observed. In this regard, future studies can work on following aspects to take CFD-based hemodynamics closer to the medical industry.

1. The integration of multiphase simulation with non-linear elastic arteries as well as non-Newtonian viscoelastic modeling remains a critical frontier, particularly in scenarios involving small hypertensive vessels. While some efforts have been made²⁴, a robust solver that considers both artery non-linearity and viscoelasticity is yet to be developed.
2. Current FSI simulations often overlook the influence of surrounding tissue on vibrations, neglecting its impact based on material properties. Future studies should delve into accounting for these effects for a more comprehensive understanding.
3. Patient-specific CAD geometries from CT images face hurdles in approval and acquisition time. While idealized models are commonly used, innovative approaches, like artificial stenosis generation (proposed in Doutel et al.⁹⁸) and neural networks offer promising avenues to create realistic yet computationally feasible models.
4. The role of various physics aspects, such as Magneto hydro dynamics (MHD)^{AL} and porous walls, remains largely unexplored in hemodynamic modeling—presenting an opportunity for deeper investigations.
5. Application of CFD models for clinical use demands less time-consuming approaches. Assessing the viability of Reduced Order Models (ROMs) for predicting hemodynamics and exploring Physics Informed Neural Networks (PINN) for multi-physics simulations could offer faster computational solutions.

Lastly, effective implementation of computational models for diagnosis and treatment heavily relies on seamless collaboration between medical practitioners and engineers. Ensuring a continuous and productive interaction between these

^{AL} Magneto hydro dynamics (MHD) is a field of study that examines the behavior of electrically conducting fluids, such as plasmas, liquid metals, or electrolytes, in the presence of magnetic fields. It combines principles from fluid dynamics, electromagnetism, and plasma physics.

domains is essential for a meaningful progress in this field. These forward-looking perspectives aim to address current limitations and pave the way for more comprehensive, clinically applicable, and efficient CFD-based hemodynamic modeling in human vasculature.

Publisher's Note

Springer Nature remains neutral with regard to jurisdictional claims in published maps and institutional affiliations.

Springer Nature or its licensor (e.g. a society or other partner) holds exclusive rights to this article under a publishing agreement with the author(s) or other rightsholder(s); author self-archiving of the accepted manuscript version of this article is solely governed by the terms of such publishing agreement and applicable law.

Data availability

The data presented here is obtained from previously published works, which are cited at appropriate locations in text.

Declarations

Conflict of interest

On behalf of all authors, the corresponding author states that there is no Conflict of interest.

Received: 13 January 2024 Accepted: 6 March 2024
Published online: 25 April 2024

References

1. Benjamin EJ, Muntner P, Alonso A, Bittencourt MS, Callaway CW, Carson AP, Chamberlain AM, Chang AR, Cheng S, Das SR, Delling FN (2019) Heart disease and stroke statistics—2019 update: a report from the American Heart Association. *Circulation* 139(10):e56–e528
2. Carvalho V, Pinho D, Lima RA, Teixeira JC, Teixeira S (2021) Blood flow modeling in coronary arteries: a review. *Fluids* 6(2):53
3. Conti M, Long C, Marconi M, Berchiolli R, Bazilevs Y, Reali A (2016) Carotid artery hemodynamics before and after stenting: a patient specific CFD study. *Comput Fluids* 141:62–74
4. Seo JH, Mittal R (2012) A coupled flow-acoustic computational study of bruits from a modeled stenosed artery. *Med Biol Eng Comput* 50(10):1025–1035
5. Zhu C, Seo JH, Bakhshae H, Mittal R (2017) A computational method for analyzing the biomechanics of arterial bruits. *J Biomech Eng* 139(5):051008

6. Ku DN (1997) Blood flow in arteries. *Annu Rev Fluid Mech* 29(1):399–434
7. Steinman DA (2002) Image-based computational fluid dynamics modeling in realistic arterial geometries. *Ann Biomed Eng* 30:483–497
8. Papathanasopoulou P, Zhao S, Köhler U, Robertson MB, Long Q, Hoskins P, Yun Xu X, Marshall I (2003) MRI measurement of time-resolved wall shear stress vectors in a carotid bifurcation model, and comparison with CFD predictions. *J Magn Reson Imaging* 17(2):153–162
9. Marshall I, Zhao S, Papanthanasopoulou P, Hoskins P, Xu XY (2004) MRI and CFD studies of pulsatile flow in healthy and stenosed carotid bifurcation models. *J Biomech* 37(5):679–687
10. Moore JA, Steinman DA, Ethier CR (1997) Computational blood flow modelling: errors associated with reconstructing finite element models from magnetic resonance images. *J Biomech* 31(2):179–184
11. Carvalho V, Rodrigues N, Ribeiro R, Costa PF, Teixeira JC, Lima RA, Teixeira SF (2021) Hemodynamic study in 3D printed stenotic coronary artery models: experimental validation and transient simulation. *Comput Methods Biomech Biomed Eng* 24(6):623–636
12. Levick JR (2013) *An introduction to cardiovascular physiology*. Butterworth-Heinemann, Oxford
13. Reid L (2021) *An introduction to biomedical computational fluid dynamics*. *Biomed Vis* 10:205–222
14. Tu J, Inthavong K, Wong KKL (2015) *Computational hemodynamics-theory, modelling and applications*. Springer, Berlin
15. Zamir M (1999) On fractal properties of arterial trees. *J Theor Biol* 197(4):517–526
16. Robertson AM, Sequeira A, Kameneva MV (2008) Hemorheology. *Hemodyn Flows* 63–120
17. Commons W Blood Vessels. Based on a diagram in my Biology textbook, and some others. https://upload.wikimedia.org/wikipedia/commons/3/3f/Blood_vessels_%28retouched%29_-en.svg
18. Pandey R, Kumar M, Majdoubi J, Rahimi-Gorji M, Srivastav VK (2020) A review study on blood in human coronary artery: numerical approach. *Comput Methods Progr Biomed* 187:105243
19. Anor T, Grinberg L, Baek H, Madsen JR, Jayaraman MV, Karniadakis GE (2010) Modeling of blood flow in arterial trees. *Wiley Interdiscipl Rev Syst Biol Med* 2(5):612–623
20. Wu J, Liu G, Huang W, Ghista DN, Wong KK (2015) Transient blood flow in elastic coronary arteries with varying degrees of stenosis and dilatations: CFD modelling and parametric study. *Comput Methods Biomech Biomed Eng* 18(16):1835–1845
21. Lorenzini G, Casalena E (2008) CFD analysis of pulsatile blood flow in an atherosclerotic human artery with eccentric plaques. *J Biomech* 41(9):1862–1870
22. Rayz VL, Bousset L, Acevedo-Bolton G, Martin AJ, Young WL, Lawton MT, Higashida R, Saloner D (2008) Numerical simulations of flow in cerebral aneurysms: comparison of CFD results and in vivo MRI measurements. *J Biomech Eng*. <https://doi.org/10.1115/1.2970056>
23. Dennis KD, Kallmes DF, Dragomir-Daescu D (2017) Cerebral aneurysm blood flow simulations are sensitive to basic solver settings. *J Biomech* 57:46–53
24. Qiao Y, Zeng Y, Ding Y, Fan J, Luo K, Zhu T (2019) Numerical simulation of two-phase non-Newtonian blood flow with fluid–structure interaction in aortic dissection. *Comput Methods Biomech Biomed Eng* 22(6):620–630
25. Chen X, Zhuang J, Huang H, Wu Y (2021) Fluid–structure interactions (FSI) based study of low-density lipoproteins (LDL) uptake in the left coronary artery. *Sci Rep* 11(1):4803
26. Wu W-T, Aubry N, Antaki JE, Massoudi M (2020) Simulation of blood flow in a sudden expansion channel and a coronary artery. *J Comput Appl Math* 376:112856
27. Bruneau DA, Steinman DA, Valen-Sendstad K (2023) Understanding intracranial aneurysm sounds via high-fidelity fluid–structure-interaction modelling. *Commun Med* 3(1):163
28. Jung J, Lyczkowski RW, Panchal CB, Hassanein A (2006) Multiphase hemodynamic simulation of pulsatile flow in a coronary artery. *J Biomech* 39(11):2064–2073
29. Xie H, Zhang Y (2017) The effect of red blood cells on blood heat transfer. *Int J Heat Mass Transf* 113:840–849
30. Ku JP, Elkins CJ, Taylor CA (2005) Comparison of CFD and MRI flow and velocities in an in vitro large artery bypass graft model. *Ann Biomed Eng* 33:257–269
31. Morab SR, Sharma A, Murallidharan JS (2024) Fully finite volume method on a curvilinear grid-based arbitrary Lagrangian Eulerian approach for computational fluid flexible-structure interaction. *Comput Phys Commun* 296:109054
32. Gidaspow D (1994) *Multiphase flow and fluidization: continuum and kinetic theory descriptions*. Academic Press, Cambridge
33. Kim YH, VandeVord PJ, Lee JS (2008) Multiphase non-Newtonian effects on pulsatile hemodynamics in a coronary artery. *Int J Numer Methods Fluids* 58(7):803–825
34. Huang J, Lyczkowski RW, Gidaspow D (2009) Pulsatile flow in a coronary artery using multiphase kinetic theory. *J Biomech* 42(6):743–754
35. Fahraeus R, Lindqvist T (1931) The viscosity of the blood in narrow capillary tubes. *Am J Physiol-Legacy Content* 96(3):562–568
36. Jung J, Hassanein A, Lyczkowski RW (2006) Hemodynamic computation using multiphase flow dynamics in a right coronary artery. *Ann Biomed Eng* 34:393–407
37. Cilla M, Pena E, Martinez MA (2014) Mathematical modelling of atheroma plaque formation and development in coronary arteries. *J R Soc Interface* 11(90):20130866
38. Pleouras DS, Sakellarios AL, Tsompou P, Kigka V, Kyriakidis S, Rocchiccioli S, Neglia D, Knuuti J, Pelosi G, Michalis LK (2020) Simulation of atherosclerotic plaque growth

- using computational biomechanics and patient-specific data. *Sci Rep* 10(1):17409
39. Filipovic N, Teng Z, Radovic M, Saveljic I, Fotiadis D, Parodi O (2013) Computer simulation of three-dimensional plaque formation and progression in the carotid artery. *Med Biol Eng Comput* 51:607–616
 40. Phillips RJ, Armstrong RC, Brown RA, Graham AL, Abbott JR (1992) A constitutive equation for concentrated suspensions that accounts for shear-induced particle migration. *Phys Fluids A* 4(1):30–40
 41. Yadav SP, Sharma A, Agrawal A (2023) Accurate modeling of blood flow in a micro-channel as a non-homogeneous mixture using continuum approach-based diffusive flux model. *Phys Fluids* 35(4)
 42. Sia SF, Zhao X, Yu Y, Zhang Y (2019) Multiphase particle-in-cell simulation in severe internal carotid artery stenosis. *Powder Technol* 358:62–67
 43. Melka B, Adamczyk WP, Rojczyk M, Nowak ML, Gracka M, Nowak AJ, Golda A, Bialecki RA, Ostrowski Z (2020) Numerical investigation of multiphase blood flow coupled with lumped parameter model of outflow. *Int J Numer Methods Heat Fluid Flow* 30(1):228–244
 44. Melka B, Gracka M, Adamczyk W, Rojczyk M, Golda A, Nowak AJ, Bialecki RA, Ostrowski Z (2018) Multiphase simulation of blood flow within main thoracic arteries of 8-year-old child with coarctation of the aorta. *Heat Mass Transf* 54:2405–2413
 45. Misra J, Adhikary S, Shit G (2007) Multiphase flow of blood through arteries with a branch capillary: a theoretical study. *J Mech Med Biol* 7(04):395–417
 46. Chien S (1970) Shear dependence of effective cell volume as a determinant of blood viscosity. *Science* 168(3934):977–979
 47. Johnston BM, Johnston PR, Corney S, Kilpatrick D (2006) Non-Newtonian blood flow in human right coronary arteries: transient simulations. *J Biomech* 39(6):1116–1128
 48. Huang C, Fabisiak W (1976) Thixotropic parameters of whole human blood. *Thromb Res* 8:1–8
 49. Braun DD, Rosen MR (2013) *Rheology modifiers handbook: practical use and application*. Elsevier, Amsterdam
 50. Rao MA (2010) *Rheology of fluid and semisolid foods: principles and applications*. Springer, Berlin
 51. Walburn FJ, Schneck DJ (1976) A constitutive equation for whole human blood. *Biorheology* 13(3):201–210
 52. Cho YI, Kensey KR (1991) Effects of the non-Newtonian viscosity of blood on flows in a diseased arterial vessel. Part 1: steady flows. *Biorheology* 28(3–4):241–262
 53. Siau W, Ng E, Mazumdar J (2000) Unsteady stenosis flow prediction: a comparative study of non-Newtonian models with operator splitting scheme. *Med Eng Phys* 22(4):265–277
 54. Quemada D (1978) Rheology of concentrated disperse systems III. General features of the proposed non-Newtonian model. Comparison with experimental data. *Rheologica Acta* 17(6):643–653
 55. Thurston GB (1979) Rheological parameters for the viscosity viscoelasticity and thixotropy of blood. *Biorheology* 16(3):149–162
 56. Oldroyd JG (1950) On the formulation of rheological equations of state. *Proc Roy Soc Lond Ser A Math Phys Sci* 200(1063):523–541
 57. Anand M, Rajagopal K (2004) A shear-thinning viscoelastic fluid model for describing the flow of blood. *Int J Cardiovasc Med Sci* 4(2):59–68
 58. Rajagopal KR, Srinivasa AR (2000) A thermodynamic frame work for rate type fluid models. *J Nonnewton Fluid Mech* 88(3):207–227
 59. Hoque SZ, Anand DV, Patnaik B (2022) A dissipative particle dynamics simulation of a pair of red blood cells in flow through a symmetric and an asymmetric bifurcated microchannel. *Comput Part Mech* 9(6):1219–1231
 60. Hoque SZ, Anand DV, Patnaik B (2018) The dynamics of a healthy and infected red blood cell in flow through constricted channels: a DPD simulation. *Int J Numer Methods Biomed Eng* 34(9):3105
 61. Fedosov DA, Caswell B, Karniadakis GE (2010) A multi-scale red blood cell model with accurate mechanics, rheology, and dynamics. *Biophys J* 98(10):2215–2225
 62. Bodnár T, Sequeira A, Prosi M (2011) On the shear-thinning and viscoelastic effects of blood flow under various flow rates. *Appl Math Comput* 217(11):5055–5067
 63. Elhanafy A, Guaily A, Elsaid A (2019) Numerical simulation of blood flow in abdominal aortic aneurysms: effects of blood shear-thinning and viscoelastic properties. *Math Comput Simul* 160:55–71
 64. Chen H, Zhong G, Li L, Chen Z, Xue Z (1988) The viscoelasticity of human blood at low shear rate. In: *Proceedings of the annual international conference of the IEEE engineering in medicine and biology society*. IEEE, pp 705–706
 65. Neofytou P (2004) Comparison of blood rheological models for physiological flow simulation. *Biorheology* 41(6):693–714
 66. Razavi A, Shirani E, Sadeghi M (2011) Numerical simulation of blood pulsatile flow in a stenosed carotid artery using different rheological models. *J Biomech* 44(11):2021–2030
 67. Arzani A (2018) Accounting for residence-time in blood rheology models: do we really need non-Newtonian blood flow modelling in large arteries? *J R Soc Interface* 15(146):20180486
 68. Abbasian M, Shams M, Valizadeh Z, Moshfegh A, Javadzadegan A, Cheng S (2020) Effects of different non-Newtonian models on unsteady blood flow hemodynamics in patient-specific arterial models with in-vivo validation. *Comput Methods Progr Biomed* 186:105185
 69. Karimi S, Dabagh M, Vasava P, Dadvar M, Dabir B, Jalali P (2014) Effect of rheological models on the

- hemodynamics within human aorta: CFD study on CT image-based geometry. *J Nonnewton Fluid Mech* 207:42–52
70. Yilmaz F, Gundogdu MY (2008) A critical review on blood flow in large arteries; relevance to blood rheology, viscosity models, and physiologic conditions. *Korea-Australia Rheol J* 20(4):197–211
 71. Morab SR, Sharma A (2020) An overview of computational fluid structure interaction: methods and applications. arXiv preprint [arXiv:2006.04068](https://arxiv.org/abs/2006.04068)
 72. Bazilevs Y, Takizawa K, Tezduyar TE (2013) *Computational fluid–structure interaction: methods and applications*. Wiley, Hoboken
 73. Bazilevs Y, Hsu M-C, Benson DJ, Sankaran S, Marsden AL (2009) *Computational fluid–structure interaction: methods and application to a total cavopulmonary connection*. *Comput Mech* 45:77–89
 74. De Hart J, Baaijens F, Peters G, Schreurs P (2003) A computational fluid–structure interaction analysis of a fiber-reinforced stentless aortic valve. *J Biomech* 36(5):699–712
 75. Michler C, Hulshoff S, Van Brummelen E, De Borst R (2004) A monolithic approach to fluid–structure interaction. *Comput Fluids* 33(5–6):839–848
 76. Hughes TJ, Liu WK, Zimmermann TK (1981) Lagrangian–Eulerian finite element formulation for incompressible viscous flows. *Comput Methods Appl Mech Eng* 29(3):329–349
 77. Trepanier J, Reggio M, Zhang H, Camarero R (1991) A finite-volume method for the Euler equations on arbitrary Lagrangian–Eulerian grids. *Comput Fluids* 20(4):399–409
 78. Hirt CW, Amsden AA, Cook J (1974) An arbitrary Lagrangian–Eulerian computing method for all flow speeds. *J Comput Phys* 14(3):227–253
 79. Peskin CS (2002) The immersed boundary method. *Acta Numerica* 11:479–517
 80. Thekkethil N, Sharma A (2019) Level set function-based immersed interface method and benchmark solutions for fluid flexible–structure interaction. *Int J Numer Methods Fluids* 91(3):134–157
 81. Xu Z, Yang Y (2020) The hybrid dimensional representation of permeability tensor: a reinterpretation of the discrete fracture model and its extension on nonconforming meshes. *J Comput Phys* 415:109523
 82. Hirschhorn M, Tchantchaleishvili V, Stevens R, Rossano J, Throckmorton A (2020) Fluid–structure interaction modeling in cardiovascular medicine—a systematic review 2017–2019. *Med Eng Phys* 78:1–13
 83. Bilgi C, Atalık K (2020) Effects of blood viscoelasticity on pulsatile hemodynamics in arterial aneurysms. *J Nonnewton Fluid Mech* 279:104263
 84. Bäumlér K, Vedula V, Sailer AM, Seo J, Chiu P, Mistelbauer G, Chan FP, Fischbein MP, Marsden AL, Fleischmann D (2020) Fluid–structure interaction simulations of patient-specific aortic dissection. *Biomech Model Mechanobiol* 19(5):1607–1628
 85. Valencia A, Munoz F, Araya S, Rivera R, Bravo E (2009) Comparison between computational fluid dynamics, fluid–structure interaction and computational structural dynamics predictions of flow-induced wall mechanics in an anatomically realistic cerebral aneurysm model. *Int J Comput Fluid Dyn* 23(9):649–666
 86. Chiastra C, Migliavacca F, Martínez MÁ, Malvè M (2014) On the necessity of modelling fluid–structure interaction for stented coronary arteries. *J Mech Behav Biomed Mater* 34:217–230
 87. Athani A, Ghazali NNN, Badruddin IA, Usmani AY, Kamangar S, Anqi AE, Ahammad NA (2021) Two-phase non-Newtonian pulsatile blood flow simulations in a rigid and flexible patient-specific left coronary artery (LCA) exhibiting multi-stenosis. *Appl Sci* 11(23):11361
 88. Born M, Huang K (1996) *Dynamical theory of crystal lattices*. Oxford University Press, Oxford
 89. Vorp DA, Rajagopal K, Smolinski PJ, Borovetz HS (1995) Identification of elastic properties of homogeneous, orthotropic vascular segments in distension. *J Biomech* 28(5):501–512
 90. Chuong CJ, Fung YC (1983) Three-dimensional stress distribution in arteries. *J Biomech Eng*. <https://doi.org/10.1115/1.3138417>
 91. Bathe K-J, Zhang H (2004) Finite element developments for general fluid flows with structural interactions. *Int J Numer Methods Eng* 60(1):213–232
 92. Zahedmanesh H, Lally C (2009) Determination of the influence of stent strut thickness using the finite element method: implications for vascular injury and in-stent restenosis. *Med Biol Eng Comput* 47:385–393
 93. Loree HM, Grodzinsky AJ, Park SY, Gibson LJ, Lee RT (1994) Static circumferential tangential modulus of human atherosclerotic tissue. *J Biomech* 27(2):195–204
 94. Nama N, Aguirre M, Ortigosa R, Gil AJ, Humphrey JD, Figueroa CA (2023) A systematic comparison between membrane, shell, and 3D solid formulations for non-linear vascular biomechanics. arXiv e-prints, 2301
 95. Solovyova H, Kizilova N, Mizerski J (2016) Nonlinear model of blood flow through stenosed coronary arteries. In: *Proceedings of the 5th international conference on nonlinear dynamics*. ND-KhPI2016
 96. Baier-Saip JA, Baier PA, Schilling K, Oliveira JC (2017) Approximate artery elasticity using linear springs. *J Med Biol Eng* 37:899–911
 97. Torii R, Oshima M, Kobayashi T, Takagi K, Tezduyar TE (2008) Fluid–structure interaction modeling of a patient-specific cerebral aneurysm: influence of structural modeling. *Comput Mech* 43:151–159
 98. Doutel E, Carneiro J, Campos J, Miranda J (2018) Artificial stenoses for computational hemodynamics. *Appl Math Model* 59:427–440



Sumant R. Morab is a PhD Research Scholar in the Computational Fluid Dynamics Lab, Mechanical Engineering Department, IIT Bombay. He specializes in Computational Fluid–Structure–Acoustic interaction solver development, with a focus

on the application of computational tools for sound-based diagnosis of stenosis and aneurysm. Mr. Morab's significant contribution lies in the development of a novel in-house Fluid–Structure–Acoustic interaction solver using hybrid grid and low-Mach approximation of acoustic equations. This solver demonstrates superior performance and lower error rates as compared to existing methods in the field. His research interests encompass the intricate interplay between fluid dynamics, structural mechanics, and acoustic phenomena—particularly in biomedical applications such as diagnosing cardiovascular conditions.



Atul Sharma is a Rahul Bajaj Chair Professor and Head of the Mechanical Department at IIT Bombay. His contributions are on development of a range of novel and efficient computational tools, their applications to numerous time-consuming simulations,

and analysis of the resulting big data for various problems in Computational Multi-Fluid Dynamics and Computational Fluid–Structure Interactions. He proposed a physical, insightful, and comprehensive approach for CFD, in his well-received textbook—to enable his vision of Make CFD Software in India! He is a Fellow of Indian National Academy of Engineering (INAE). His wide variety of research is

published with 122 articles in 44 different well-recognized international journals, 85 conference proceedings, and 14 chapters in 5 edited books, and appeared in cover page of top-class journals (Journal of Fluid Mechanics, Physics of Fluids, and Langmuir). He contributed as a CFD consultant at Global R &D, Crompton Greaves Limited, Mumbai, served as Secretary, National Society of Fluid Mechanics and Fluid Power, and presently an associate editor for 3 international journals. He received “IIT Bombay Departmental Award for Excellence in Teaching 2019” and “IIT Bombay Research Dissemination Award 2020”.



Janani S. Murallidharan is an Associate Professor at the Mechanical Engineering Department at IIT Bombay. She has completed her Ph.D. in Mechanical Engineering from Indian Institute of Technology, Madras. Prior to this, she has done her B.E.

in Mechanical Engineering from Hindustan College of Engineering, Anna University, India, followed by a M.E. in Aerospace Engineering at Iowa State University. She was a researcher in the Mechanical Engineering Department at Imperial College London until December 2015. Both at IIT Madras and at Imperial College London she has been part of several Multiphase Heat Transfer research projects. At IIT Bombay, Prof. Murallidharan specializes in the areas of computational fluid dynamics, multiphase flow and heat transfer, Bio-fluid dynamics, and phase change phenomenon. Her current research interests are in the areas of boiling, and bubble contact line dynamics, blood flow modeling, and CFD-based ventilation studies.